

Engineered In vitro Models for Pathological Calcification: Routes Toward Mechanistic Understanding

Elham Radvar, Gabriele Griffanti, Elena Tsolaki, Sergio Bertazzo, Showan N. Nazhat, Owen Addison, Alvaro Mata, Catherine M. Shanahan, and Sherif Elsharkawy*

Physiological calcification plays an essential part in the development of the skeleton and teeth; however, the occurrence of calcification in soft tissues such as the brain, heart, and kidneys associates with health impacts, creating a massive social and economic burden. The current paradigm for pathological calcification focuses on the biological factors responsible for bone-like mineralization, including osteoblast-like cells and proteins inducing nucleation and crystal growth. However, the exact mechanism responsible for calcification remains unknown. Toward this goal, this review dissects the current understanding of structure–function relationships and physico-chemical properties of pathologic calcification from a materials science point of view. We will discuss a range of potential mechanisms of pathological calcification, with the purpose of identifying universal mechanistic pathways that occur across multiple organs/tissues at multiple length scales. The possible effect of extracellular components in signaling and templating mineralization, as well as the role of intrinsically disordered proteins in calcification, is reviewed. The state-of-the-art in vitro models and strategies that can recreate the highly dynamic environment of calcification are identified.

of calcium minerals on soft tissues known as pathologic calcification creates the basis of severe diseases. Calcification in soft tissues leads to many extra-skeletal diseases including calcification in hemodialysis patients, calcific aortic stenosis, atherosclerosis, kidney and bladder stones, dental pulp stones, some gall stones, salivary gland stones, chronic calculous prostatitis, testicular microliths, some dementias, calcinosis cutis, several malignancies, calcific tendinitis, synovitis, arthritis, and cancerous tumors.^[1]

Pathological calcification is part of high mortality diseases, such as cardiovascular diseases with 17 million deaths per year (reported in 2008)^[2] and 42% mortality rate in low-income and 28% in high-income European countries (reported in 2012 and 2019)^[3,4] comprising 19% of total health-care expenditure in European countries (recent report in 2019).^[4] For example, calcific aortic valve disease leads to heart failure in 50% of patients over the age of 85.^[2]


Moreover, the atherosclerotic calcified plaques is a highly prevalent disease, affecting about 65% of the population over the age of 40, where the current treatment involves valve replacement surgeries with 3% rate of mortality.^[2,5] On the other hand, urinary tract calcification, known as kidney stones, is a worldwide problem affecting 15% of population in developed

1. Introduction

Hard tissues in human body consist of mineral phase that is mostly composed of hydroxyapatite (HAp) and is the primary mineral in bone and teeth.^[1] However, the abnormal deposition

Dr. E. Radvar, Prof. O. Addison, Dr. S. Elsharkawy
Centre for Oral, Clinical and Translational Sciences
Faculty of Dentistry, Oral and Craniofacial Sciences
King's College London
London SE1 1UL, UK
E-mail: sherif.elsharkawy@kcl.ac.uk

Dr. G. Griffanti, Prof. S. N. Nazhat
Department of Mining and Materials Engineering
Faculty of Engineering
McGill University
Montreal, QC H3A 0C5, Canada

 The ORCID identification number(s) for the author(s) of this article can be found under <https://doi.org/10.1002/anbr.202100042>.

© 2021 The Authors. Advanced NanoBiomed Research published by Wiley-VCH GmbH. This is an open access article under the terms of the Creative Commons Attribution License, which permits use, distribution and reproduction in any medium, provided the original work is properly cited.

DOI: 10.1002/anbr.202100042

Dr. E. Tsolaki, Dr. S. Bertazzo
Department of Medical Physics and Biomedical Engineering
University College London
London WC1E 6BT, UK

Prof. A. Mata
School of Pharmacy
University of Nottingham
Nottingham NG7 2RD, UK

Prof. C. M. Shanahan
BHF Centre of Research Excellence
Cardiovascular Division
James Black Centre
King's College London
London SE1 1UL, UK

countries with a high rate of recurrence, close to 50%.^[6] Despite the presence of highly advanced clinical and surgical treatments for calcifications such as arterial plaques and kidney stones, the challenges for preventing the complications of stenting for atherosclerosis patients and the recurrence of kidney stones drive the scientists to offer efficient solutions.^[2,5,6]

Brain calcification is vastly common in patients with neurological or metabolic disorders, where 20% of cases are among the elderly revealing in clinical manifestations as tremors, parkinsonism, seizures, and dementia.^[7] The susceptibility of brain tissues to calcium deposition is not clear; however, the genetic factors seem to play an important role.^[8] In brain tissue calcifications, the presence of osteogenesis markers was depicted in calcified vasculature regions.^[9] Studies on patients suffering from Parkinson's and Alzheimer's diseases exhibited α -Synuclein-positive structures.^[10] Being an IDP, α -Synuclein structures drive the attention toward the intermolecular interactions of IDPs, which occur at the protein–mineral interface.^[11] The mineral characterization has provided lots of information on the calcification process in the cardiovascular system and kidney stones. Similar approaches have been applied for studying the calcification in brain, breast cancer, and other soft tissues over the past two decades. The opportunity that material science offers in expanding the understanding of calcification can lead to the emergence of more effective therapies in calcification-related diseases.

Toward this goal, various research groups are designing materials that exhibit functionalities from disordered proteins such as elastin^[12,13] and collagen^[14,15] known to be involved in pathologic calcification.^[12] This will not only allow us to study the structural properties of those calcified tissues and pursue further mechanistic understanding of the disease but also provide novel personalized and preventive treatment for those disorders. This review aims at looking into mechanisms of calcification in pathologically calcified tissues (cardiovascular system, kidney, and brain), through the intracellular and extracellular factors, to bridge the clinical analysis into in vitro model developments (Figure 1).

2. Phase Composition and Structural Analysis

Soft tissue calcification is a highly dynamic and complicated process, where its structure–function relationship is not yet fully understood.^[16] On the other hand, the hierarchical structure of the human bone and teeth tightly associates with its function, which has been well studied.^[16–18] Therefore, studying the mineralization pattern and structure in bones and teeth would facilitate our understanding of the formation and growth of calcified deposits.^[5] Furthermore, understanding the calcified lesions in soft tissues would provide vital knowledge about the structure of minerals formed throughout the calcification process.^[19]

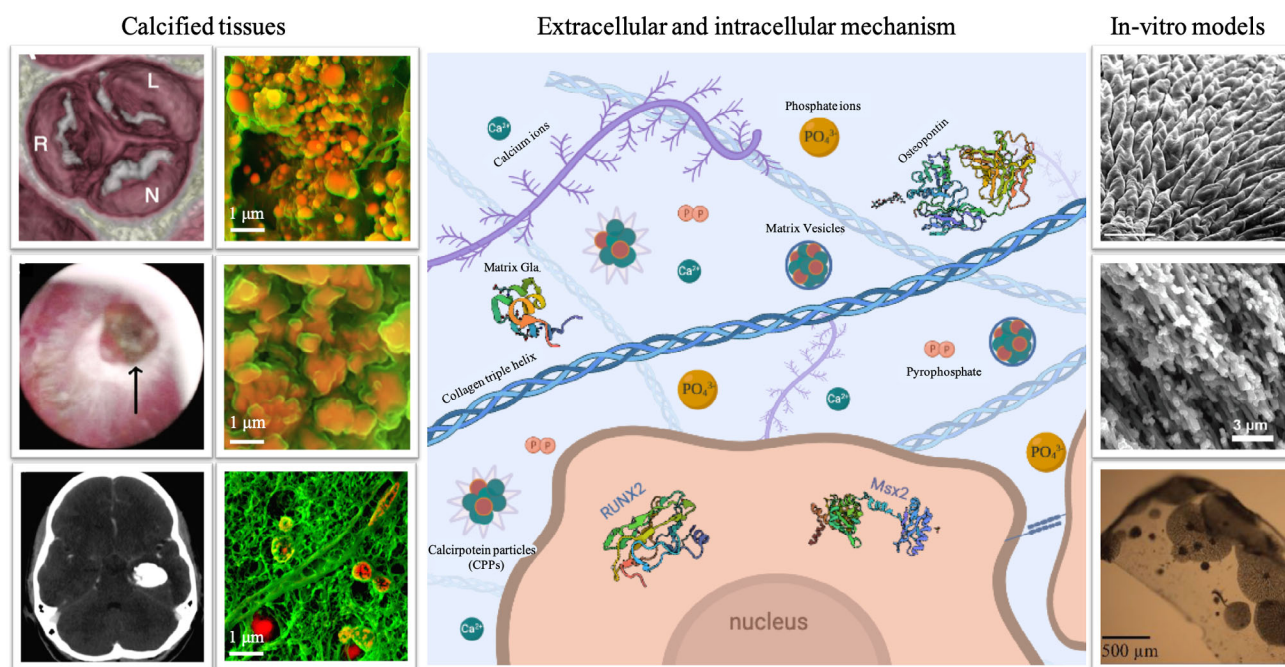


Figure 1. Top left: calcification in right (R), left (L) coronary and noncoronary (N) leaflet shown by three-dimensional (3D) contrast-enhanced computed tomography (CT) reconstructions of TAVI patients. Reproduced with permission.^[24] Copyright 2019, BMJ Publishing Group Ltd. Middle left: endoscopic image of HAp deposits in renal papillae. Reproduced with permission.^[56] Copyright 2013, Springer Nature; Bottom left: large calcified mass in the left temporal lobe seen in skull X-ray. Reproduced with permission.^[60] Copyright 2013, Springer Nature; scanning electron microscopy image and density-dependent color scanning electron micrographs (DDC-SEM) of calcified cardiac tissue, kidney biopsy. Reproduced with permission.^[160] Copyright 2016, Elsevier, and brain calcification; schematic of extracellular and intracellular factors in pathological calcification (Created with BioRender.com); Top right: prism-like mineralized structures on elastin membrane. Reproduced with permission.^[12] Copyright 2018, Springer Nature. Middle right: mineralized collagen film. Reproduced with permission.^[161] Copyright 2012, American Chemical Society and Bottom right: light microscopy image of mineralized elastin membrane. Reproduced with permission.^[12] Copyright 2018, Springer Nature.

This would further define the mechanical and functional properties of calcified tissues.^[16]

2.1. Cardiovascular Calcification

Cardiovascular calcification is one of the underlying reasons for several high-mortality diseases including atherosclerosis,^[20] calcific aortic valve disease,^[21] and chronic kidney disease (CKD).^[22,23] Currently, there are no treatments and prevention for cardiovascular calcification, to reverse the formation of calcified deposits leading to atherosclerosis.^[24,25] Even though the calcified valves can be replaced by prosthetic implants, these treatments suffer from a high death rate or implant rejection by the host body.^[26,27] One way to better understand the mechanism of calcification in the cardiovascular system is to study the structure and physico-chemical properties of the calcified deposits and in relation to the extracellular matrix (ECM) of the tissues.^[28] The multidisciplinary approach would benefit us in analyzing these minerals using advanced imaging and spectroscopic techniques that are widely applied in materials science research.

2.1.1. Composition and Nanoscale Architecture of Calcified Soft Tissue

Applying the structural analysis approaches that are routinely utilized to study the bone structure, including advanced microscopy and spectroscopy techniques, such as scanning electron microscopy (SEM – nano/micrometer resolution imaging),^[2,27,29] transmission electron microscopy (TEM – angstrom/nanometer resolution imaging),^[2,16] selected area electron diffraction (SAED – crystallographic structure),^[2,16] and energy-dispersive X-ray spectroscopy (EDS – elemental analysis),^[2,27] would be highly beneficial in understanding the structure–function relationship of pathological calcification.^[16] Scrutinizing the composition and structural characteristics of calcified deposits provides important information about the mechanism of calcification, which can be compared with native bone structure.^[16,19] This is essential in finding novel treatments and techniques for preventing and treating diseases that arise from pathological calcification.

As one of the most common tissues prone to calcification, the human aortic valve is under high risk of calcification as we age.^[16,30] Even though bioprosthetic heart valves made from porcine and bovine heart tissues have been used as an alternative replacement, but they are reported to calcify over time.^[31] Structural characterization of calcified human aortic valves by SEM showed three structural patterns, including spherical particles (Figure 2A), fibers (Figure 2B), and compact calcification (Figure 2C) areas.^[2,16] In both natural and prosthetic valves, spherical crystalline deposits are evident, as they spread over the surface of the tissue.^[29] The crystalline structures revealed in the calcific deposits are arranged into aggregates (1–10 μm), large nodules (20–30 μm), and sheets that are organized alongside the matrix fibrils in the form of fine microcrystalline needle-like structures and aggregates.^[32] Calcification in the natural heart valve also showed spherical morphology, which covers the surface of the tissue.^[29] The spherical particles contain

calcium and phosphorus, with sizes ranging from 100 nm to 5 μm, that are not previously seen in the bone structure.^[2] They share some morphological similarities with matrix vesicles (MVs) (membrane-bound spherical structures) to some extent, but are not quite associated with MVs as they tend to be in large sizes and dense structures.^[2] Bertazzo et al. performed chemical analysis on calcified aortic valves using delicate sectioning with a focused ion beam (FIB) to examine the internal section by TEM with EDS and SAED.^[2] The analysis revealed that calcium and phosphorus were abundant in the internal section of the calcified lesions with a small amount of magnesium embedded therein (Figure 2D,E).^[2] The internal structure of particles composed of concentric and unfaceted mineral layers of varying electron density with electron diffraction patterns of highly crystalline HAp (Figure 2F–H).^[2] Even though most of the calcific lesions show similar composition to lamellar bone composed of calcium, phosphorus, and oxygen, but bones lack magnesium and present a different structure.^[2] The size of spherical particles can be correlated with the severity of the disease.^[2]

2.1.2. Structure and Composition of Bone for Comparison

Bone as an impressive biological hard tissue, comprising of hierarchical self-assembled structures that provide its stiffness and toughness.^[33] The hierarchical mineral organization of bone mainly categorizes as longitudinal (filamentous), out of plane (or lacy) and hexagonal structures (rosette).^[33] The role of collagen matrix in directing the mineral crystallization is widely reported.^[33–35]

Studying the well-established structure of bone show apatite crystals covering the fibrillar structures of collagen (Figure 2I,J).^[36] However, the calcific lesions have been shown to be independent from interaction with collagen fibers and rather stand isolated and maintain their structures (Figure 2K,L).^[16] In calcified lesions, the mostly found structures are spherical particles (Figure 2K), with calcified fibers and compact calcification depositing after spherical particles in abundance.^[16] Only 13% of the calcific lesions are reported to resemble bone structure with lamellar bone features, and the majority are likely resulted from dystrophic mineralization.^[16] Calcific lesions do not follow the nanoorganization of bone and their mineral structure is rarely crystalline. In the analysis performed by Duer et al.,^[37] typical ¹³C solid-state nuclear magnetic resonance (SSNMR) spectra revealed that the collagen signals overtake the SSNMR spectra of bone (Figure 2M). The characteristic peaks at 76 and 103 ppm corresponding to glycosaminoglycans (GAGs) backbone are predominant in mineralized plaque.

2.1.3. Dystrophic and Osteogenic Calcification and Nodules

The type of calcification, being ectopic or dystrophic, depends on the mechanical stress and proinflammatory factors. As an example, the calcification in aortic valve is mostly dystrophic calcification, displaying disturbed organization of elastin, lipid depositions, chronic inflammation, fibrosis, spotted calcium deposits, macrophage, and T-lymphocyte infiltration.^[38] The calcification in aortic valve leaflet presents itself in the form of nodules that are rich in calcium deposits.^[27] The dystrophic

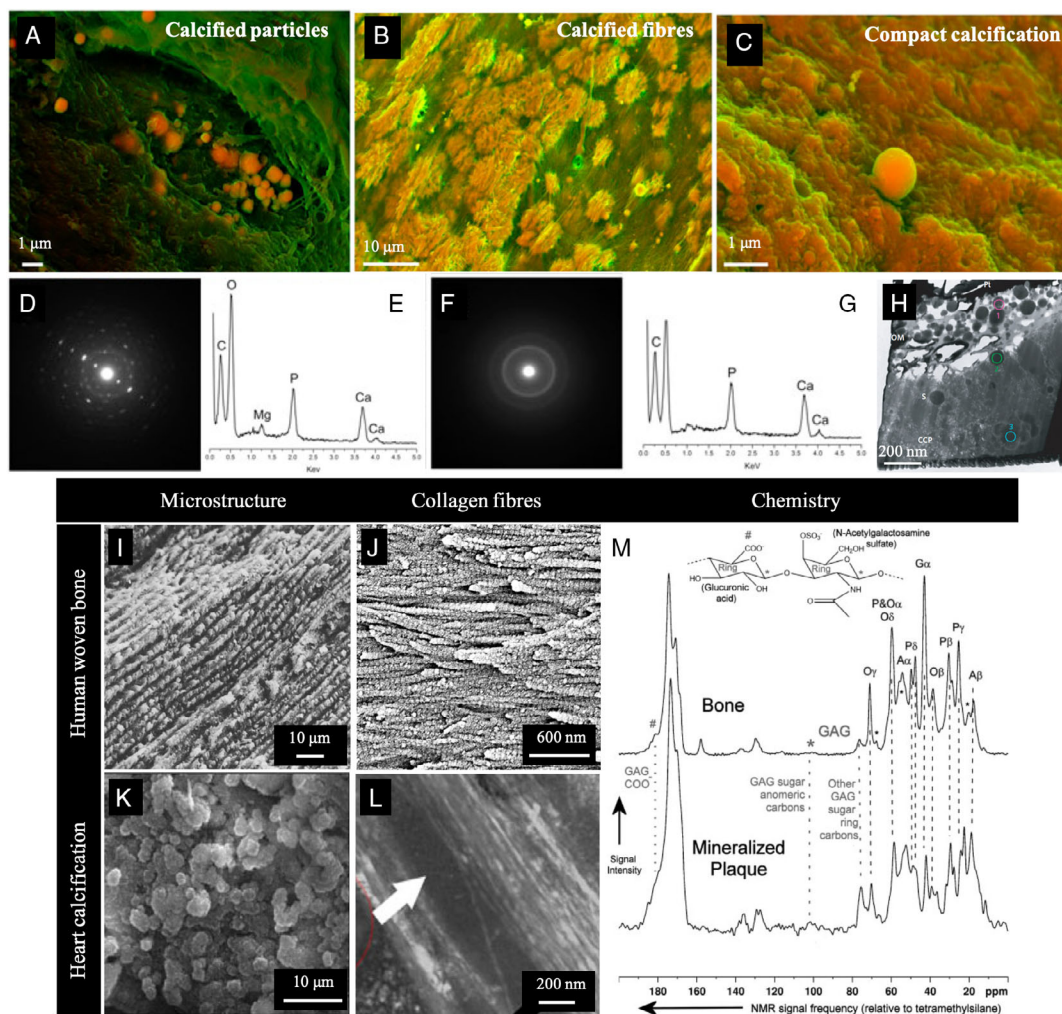


Figure 2. Representative DDC-SEM micrographs of A) calcified particles, B) calcified fibers, and C) compact calcification with a calcified particle in human aortic valve tissue. Reproduced with permission.^[16] Copyright 2016, Oxford University Press. SAED images of a calcified spherical particle (D) with its EDX analysis (E) and compact calcification with a typical amorphous pattern (F) and its EDX analysis (G) showing that it is composed of calcium, phosphorus, and magnesium. TEM images show spherical particles (S) trapped in compact calcium phosphate (CCP) and organic matrices (OM) (H). Reproduced with permission.^[16] Copyright 2016, Oxford University Press. Comparison of bone and heart mineralization: human woven bone: lamellar microstructure (I). Reproduced with permission.^[162] Copyright 2014, Elsevier and organization of apatite crystals and collagen fiber (J). Reproduced with permission.^[36] Copyright 2003, Elsevier; heart calcification: SEM of calcified heart valve (K). Reproduced with permission.^[29] Copyright 2010, John Wiley and Sons, TEM of compact calcification in human aortic valve calcification that collagen fibers are indicated with black arrow (L). Reproduced with permission.^[16] Copyright 2016, Oxford University Press and comparison of 13C spectra of mineralized plaque and bone (M). Reproduced with permission.^[37] Copyright 2008, Wolters Kluwer Health, Inc.

calcification can be identified with amorphous and crystalline deposits, in which the osteogenic calcification is present in 13% of calcified valves showing the presence of osteoid matrix (similar to mature bone formation).^[27] One method to distinguish the two types of calcification from each other is by scrutinizing the calcified nodules in the calcified tissue.^[21] In the aortic valve calcification, the hard body containing calcium phosphate phases is named as calcified nodules observed on the fibrosa layer of aortic valve leaflets.^[27,39] In vitro models of valvular calcification cleared out the differences in the dystrophic and osteogenic nodules that are formed in the presence of TGF-β1 and have rather similar morphology similar to cellular aggregates but differ in the mechanism of formation.^[27] Dystrophic nodules

are more evident in dead cells, where they have a role in directing the differentiation of aortic valve interstitial cells (AVICs) toward myofibroblasts through inflammatory cytokines pathway.^[40,41] In contrast, osteogenic nodules are formed via osteogenesis of AVIC-secreting bone matrix components.^[21,27]

Calcified nodules are in the form of aggregates with elongated cells in a radial pattern in dystrophic model and aggregates with flattening cells lining along the aggregates in osteogenic model.^[27] Moreover, the size of calcified nodules is varied depending on dystrophic or osteogenic models and are generally larger in dystrophic nodules.^[27] The calcium and phosphorus levels are higher on the surface of the nodules in osteogenic compared to dystrophic models, where the calcification is

concentrated in deeper regions of nodule.^[27] This difference of calcium and phosphorus concentrations on the surface of nodules reveals information on type of calcification (dystrophic or osteogenic), which can be used as a model to study the effective factors in mineralization.^[27,42]

The type of cells in aortic valves can play an important role in its maintenance and function.^[43] For example, valvular interstitial cells (VICs) are the most abundant type and have been targeted as a model for studying in vitro aortic valve calcification.^[39] The rationale behind the use of VICs as calcification models is their trans-differentiation to bone-forming cells that mediate the calcification process.^[39] However, the environment of the VICs is also effective in their calcification behavior. For example, a study by Cloyd et al. confirmed the presence of TGF- β 1 in osteogenic medium may induce the collagen secretion compared to spontaneous deposition of calcified nodules in control medium.^[39] This observation showed that the calcification process is more controlled in the osteogenic medium containing TGF- β 1. In another study, the effect of TGF- β 1 is tested alongside the mechanical strain on forming of calcified nodules,^[25] which also confirmed the increased numbers of calcified nodules with increasing concentrations of TGF- β 1. Nevertheless, the stimulation of TGF- β 1 is highly dependent on the substrate stiffness, and this should be considered in choosing in vitro models for studying calcification.^[25] The kinetics of calcific nodule formation revealed that the cell aggregates develop necrotic cells toward the center of aggregate and apoptotic cells cover the ring around the periphery of the nodule.^[25]

2.1.4. Physio-Chemical Properties of Calcification

The physio-chemical process of crystal nucleation in living organisms is highly regulated by cellular and extracellular molecules.^[15] However, studying the mineral growth phase is essential in proposing possible mechanism of calcification.^[44] The crucial aspect in mineralization is the initiation of the nucleation points, which requires the highest energy,^[15] and once a nucleus forms, the growth of crystals takes place with lower energy levels by ion addition.^[15]

The inorganic calcium orthophosphate consists of calcium, phosphorus, and oxygen. Among the minerals phases, carbonates are present as substituent anions for phosphates known as B-type substitution, whereas smaller percentages of this substitution by magnesium increases the solubility.^[45]

Biological apatite has platelet-like crystals (elongated along the crystallographic c-axis of collagen fibrils) with small dimensions and narrow in thickness. In contrast, the minerals in pathological calcifications mostly occur as single or mixed phases of calcium orthophosphates (amorphous calcium phosphate – ACP, dicalcium phosphate dihydrate – DCPD, octa-calcium phosphate – OCP, and β -tricalcium magnesium phosphate), magnesium orthophosphates, calcium pyrophosphates, and calcium oxalates.^[45] Among all mineral phases, the most commonly reported precursor is HAp, followed by ACP, brushite (DCPD, $\text{CaHPO}_4 \cdot 2\text{H}_2\text{O}$), monetite (dicalcium phosphate anhydrous (DCPA), CaHPO_4), and finally OCP ($\text{Ca}_8\text{H}_2(\text{PO}_4)_6 \cdot 5\text{H}_2\text{O}$).^[32]

Investigating the mineral surface and components in calcified plaques^[37] and cardiovascular deposits^[46] using nuclear

magnetic resonance (NMR),^[37] X-ray diffraction (XRD),^[32,37,46] and Fourier transform infrared spectroscopy (FTIR)^[32,46] techniques showed that the majority of initial inorganic phase of calcification is a poorly crystalline carbonated apatite of B-type, where CO_3^{2-} partly substitutes the PO_4^{3-} sites. Furthermore, Ca-P phases have been identified at initial stages of mineralization as ACP, OCP, DCPD, and magnesium-substituted β -tricalcium phosphate.^[44] Pilarczyk et al.^[47] showed the growth of calcium minerals in human aortic valves using Raman microimaging from the initial state of OCP-like deposits up to maturation to HAp state. In EDX analysis of bioprosthetic valves, components of calcification were detected as calcium and phosphorus in an atomic ratio of 1.675, and the presence of magnesium with a definite correlation with calcium reveals a significant role of magnesium in calcification of valve tissue.^[32] It is reported that the magnesium occurs mostly in the early stages of calcification in a way that stabilizes amorphous calcium phosphate in the vesicles, where the nucleation initiates.^[32]

Recognition of mineral phases is carried out either microscopically due to birefringence properties of oxalate and pyrophosphate or by hematoxyphilia for apatite and carbonate mineral phases.^[48] Although the presence of whitlockite in medial calcification of aorta being invisible to histologic methods, it is characterized by XRD and EDX.^[48] The formula of whitlockite, $\text{Ca}_9\text{MgH}(\text{PO}_4)_7$, that is a magnesium-substituted calcium phosphate, and it is referred to as β -TCP due to their similar XRD patterns and or insolubility in acetic acid but in water.^[48] In whitlockite, the ratio of hydrogen phosphate to phosphate is 1:6, and Mg^{2+} and HPO_4^{2-} play an important role in its structure, whereas these two ions are absent in β -TCP.^[49,50] At a maturation state of calcification, carbonated apatite and whitlockite are reported in human cardiovascular tissue.^[51,52] Whitlockite occurs in renal calculi with other phases of minerals such as calcium oxalate, struvite, and apatite.^[49] Analysis of crystal nucleation and growth is beneficial in greater understanding of calcification mechanism, which may lead to effective therapies and treatments.

2.2. Kidney Stones

Kidney stone formation, being a complex process, can be induced by several factors including genetic disorders, metabolic imbalances, dietary, and lifestyle.^[6,53] Analysis of the structure and composition of kidney stones would benefit the field by not only providing the mechanisms of mineral formation but also the tools for advanced and effective treatments.

However, the multicomponent nature of kidney stones as mixtures of oxalates, phosphates, and urates is challenging for quantitative analysis.^[54] Therefore, advanced analysis techniques are required to be applied in kidney stone characterization.

2.2.1. Structural Characterization

Uroliths known as a condition of kidney stone formation, affecting 5% of industrialized population, with two common treatments; percutaneous nephrolithotripsy and extracorporeal shockwave lithotripsy (ESWL).^[55] The structural composition of the kidney stone provides information on its mechanical

properties, including the hardness, which indicates the efficacy of the ESWL treatment.^[55] Better understanding of the mechanical response of the kidney stones would lead to the best parameters for ESWL and minimizes the side effects.^[55]

Smaller sizes of uroliths are called papillary renal calculi that form 13% of renal calculi.^[56] These types of renal calculi have a concave face adjacent to the renal tissue and an opposite convex face.^[56] The concave zone can be heterogeneous in the size of calcified lesions, consisting from small HAp residues to Randall's plaques (well-developed HAp plaques) (Figure 3A1).^[56,57] Two structures are identified for the internal section of kidney stones,

including the laminar structure with no evidence of nucleus, and the crystalline matrices that are anisotropically distributed with either a central or peripheral nucleus.^[55]

The main mineral reported in renal calculi is calcium oxalate monohydrate (COM, $\text{CaC}_2\text{O}_4 \cdot \text{H}_2\text{O}$) along with HAp, which has been identified in the core of the mineral. Moreover, three main compositions are identified in kidney stones as uric acid (UA, 15%) (Figure 3A2), calcium oxalates (63–69%) (Figure 3A3), and magnesium ammonium phosphate hexahydrate (MAPH, 10–20%).^[53,55] Depending on the composition of kidney stones, they can adopt different structures. For example, in uric

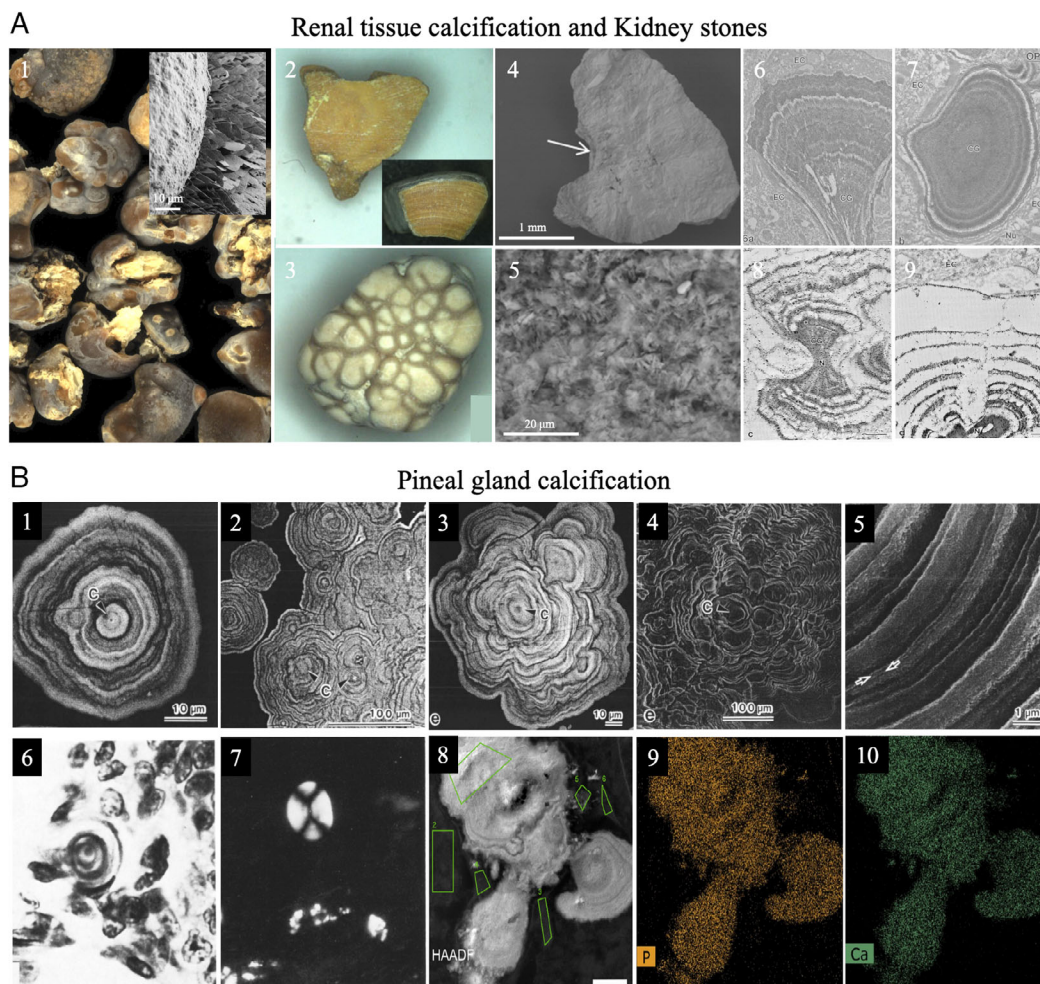


Figure 3. Types of mineralization in renal tissue (A). Typical monohydrate calcium oxalate stones harboring papillary umbilication and Randall's plaque made of apatite (white structures) (1), Insert: SEM of the interface between Randall's plaque made of apatite (foreground) and stone made of monohydrate calcium oxalate (background). Reproduced with permission.^[57] Copyright 2019, MDPI, patient's kidney stone samples: uric acid group with its cross section (insert) (2) and calcium oxalate group (3). Reproduced with permission.^[55] Copyright 2011, Springer Nature, SEM images of COM papillary calculi, type IV calculus in which the core, situated near the concave zone (arrow) (4 and 5). Reproduced with permission.^[56] Copyright 2013, Springer Nature; Electron micrograph of crystal ghosts (CGs) of larger stones with concentric lamellae labeled for OPN (6 and 7), in renal calculi growth, the OPN-containing lamellae (asterisks) are arranged concentrically around a nucleus (N) (8 and 9). Reproduced with permission.^[58] Copyright 2009, John Wiley and Sons. Pineal gland calcification (B). Backscattered electrons (BSE) images of ground surfaces of pineal concretions. Simple (1 and 2) and scallop-shaped (3) concentric laminations around the calcospherulite center, SEM images of ground surfaces of pineal concretions showing scallop-shaped laminations (4 and 5). Reproduced with permission.^[64] Copyright 1994, Oxford University Press, calcareous concretion (HE) in the encapsulating tissue of the pineal exhibiting the commonly observed concentric layers (6), polarization micrograph of a peripineal acervulus (unstained) showing the typical Maltese cross (7). Reproduced with permission.^[63] Copyright 1969, Springer Nature. SEM/EDX analysis of the same brain region (8), phosphorus mapping (9), and calcium mapping (10). Reproduced with permission.^[8] Copyright 2018, Elsevier.

acid-based samples, homogenous microstructures with concentric laminar rings are evident.^[55] On the other hand, in the kidney stones with calcium oxalate mineral composition, two distinct regions of globular and laminar internal structure and white powdery external structure are common.^[55] During renal calculi formation, McKee and colleagues showed the organization of osteopontin (OPN) throughout this process.^[58] Through electron micrographs, the calculi formation is evidenced as “crystal ghost” (CG) that immunodetecting labeling showed the presence of OPN in concentric order around a nucleus (Figure 3A6–9).^[58]

The main difference of calcium oxalate compared to the other composition types is its hydration ratio, which is the number of water molecules per calcium oxalate molecule. This hydration ratio affects the thermal decomposition of these type of stones. In nature, calcium oxalate crystals form either as COM (Figure 3A4,5)^[56] or calcium oxalate dihydrate (COD, $\text{CaC}_2\text{O}_4 \cdot 2\text{H}_2\text{O}$), and the calcium oxalate stones contain both types in mixed quantities.^[55] Magnesium ammonium phosphate hexahydrate is the third common composition found in kidney stones and often composed of a thick opaque brown outer layer with white center.^[55] The heterogeneity of the structures of uroliths is due to the long period of time of their formation. The calcified lesions grow larger in the collagen-rich regions and near the vasa recta or the thin-loop basement membranes.^[56]

2.2.2. Mineral Phase Composition

The morphology of kidney stones highly depends on the pH of the environment and the growth process, where each particular structure can be indicative of a given disease.^[6] The crystal structure of the majority of minerals in kidney stones is rather monoclinic or orthorhombic, meaning that they have lower crystal symmetry.^[54] The appearance of kidney stones exhibits more or less clear zonality such as, concentric layers, lamellar structure, and breccia-like structure.^[54] Powder XRD and FTIR are widely used in identifying crystalline phases, and the most common minerals in kidney stones are whewellite (COM), uric acid ($\text{C}_5\text{H}_4\text{N}_4\text{O}_3$), weddellite (COD), brushite (calcium hydrogen phosphate dihydrate – BRS, $\text{CaHPO}_4 \cdot 2\text{H}_2\text{O}$), struvite (magnesium ammonium phosphate hexahydrate – SV, $\text{MgNH}_4\text{PO}_4 \cdot 6\text{H}_2\text{O}$), HAp, carbonated HAp (CAP, $\text{Ca}_5(\text{PO}_4)_3\text{OH}$), uricite (anhydrous uric acid – UAA, $\text{C}_5\text{H}_4\text{N}_4\text{O}_3$), uric acid dihydrate (UAD, $\text{C}_5\text{H}_4\text{N}_4\text{O}_3 \cdot 2\text{H}_2\text{O}$), and ammonium acid urate (AAU, $\text{NH}_4\text{C}_5\text{H}_3\text{N}_4\text{O}_3$).^[6,54]

Kidney stones rich in uric acid show no traces of calcium or phosphorus in EDS spectra, and their elemental peaks consist of C, N, and O (endothermic peak at 450).^[55] On the other hand, kidney stones rich in calcium oxalate, due to their water crystal phases, their thermogravimetric analyses reveal three steps of mass losses corresponding to 12% loss in the first step at 200 °C, second step of mass loss at 400 °C, and 26% loss of carbon dioxide at 740 °C in the third step.^[55] The EDS evaluation of internal composition showed traces of Ca, C, and O, and the external powdery form contains calcium phosphate due to phosphorus traces.^[55] The MAPH decomposition is lower than the other two, around 160 °C; however, full mass loss is not achievable as the calcium phosphate is resistant at higher temperatures.

Nevertheless, elemental analysis of the exterior and white interior showed that the outer layer is formed by calcium oxalate and the interior revealed C, O, Ca, P, and Mg peaks.^[55] Based on XRD data, uroliths exhibit lower crystallinity and traces of other minerals such as calcium oxalate dihydrate, CaCO_3 , and even sodium chloride.^[53] FTIR analyses of kidney stones provide compositional data of the renal calculi structure, revealing the vibrational stretches corresponding to specific mineral phases, such as characteristic band of oxalate group in COM, phosphate bands of HAp, and C–O vibration in AAU.^[6] In the SEM analysis of COM crystals, plate-like morphology randomly oriented are more evident, whereas in stones with major composition of UAA (≈ 98 wt%), rhomboidal blocks of uric acid crystals are more visible.^[6] Among the crystals, HAp formed the smallest crystallite size.

2.3. Brain Calcification

Brain calcifications can occur in different regions, such as basal ganglia, thalamus, hippocampus, and cerebellum. Calcification is found in patients with a neurodegenerative disease, the familial idiopathic basal ganglia calcification (FIBGC) known as Fahr’s disease that shows symmetric calcifications of the basal ganglia, thalamus, and cerebellum.^[8,59] The genetic disease of FIBGC is based on mutations in SLC20A2 encoding inorganic phosphate transporter (PiT2), with several studies focusing on the role of PiT2 in this type of calcification.^[59] In recent decades, the progress in imaging modalities especially cross-sectional CT make it possible to identify intracerebral calcification.^[60] Brain stones or cerebral calculi are hard bone-like tissues that are mostly seen in patients with seizures; they can be extra- or intra-axial in organization.^[60] Imaging techniques are of great importance in finding and diagnosing brain calcification that can be useful in understanding the mechanism of calcification to offer efficient treatments.

2.3.1. Pineal Gland Calcification

Mineralization in the pineal gland is commonly observed as “calcospherites,” where they can partially or fully cover the gland.^[61] It has been found in 53% of lateral skull radiographs, even though it has been considered as a physiological phenomenon, it also occurred in pineal tumors.^[62] Early observations of dried pineal gland with microscopes revealed that the gland conchoidally fractured under pressure and mulberry-like surfaces were exposed.^[61,63] While a polarized light microscopy was used on concretions, distorted Maltese crosses were observed,^[63] indicating the presence of aggregations of several microscopic crystals.^[61] SEM analysis of fractured crystals showed small needle-like crystals similar to those observed in calcified plaques in human aortas.^[61] Scanning electron analysis of pineal concretions revealed two simple and scallop-shaped calcospherulite structures (Figure 3B1–5).^[64] The sectioning of the concretions revealed flat structures, which using naphthal hydroxamic acid (Na) staining showed the uneven scattering of calcium within the concretions (Figure 3B6,7).^[63] Microstructural analysis on calcified region in the brain showed similar distribution of

calcium and phosphorus in EDX mapping of calcified brain (Figure 3B8–10).^[8]

While the role of pineal gland in controlling the directional sense is not clear, studies on patients with a lower sense of direction showed pineal gland calcification in skull radiographs.^[62] The high concentrations of magnetite found in the base of skull around the sphenoid-ethmoid sinus complex have raised questions on the effect of magnetite on the mechanism of pineal gland calcification.^[62] Further analysis of human brain tissue showed the presence of magnetite (Fe₃O₄) around the cerebral lobes, cerebellum, basal ganglia, and midbrain.^[65] The nanoscale dimensions of these magnetite particles and prismatic crystal shapes indicate that they are formed through biological processes.^[66] There is a correlation between the concentration of magnetite in human brain and prevalence of Alzheimer's disease (AD).^[66] Formation of senile plaques containing β -amyloid fibrils as early symptoms of AD is associated with occurrence of damaging reactive oxygen species through redox-active transition metal ions.^[66] The effect of magnetite is rather negative on enhancing the toxicity of β -amyloid.^[66]

2.4. Other Calcification Sites

Unlike physiological mineralization, calcification in soft tissues can occur on undesired sites and leads to many extra-skeletal diseases. We mentioned three widely studied areas in previous sections, but calcification can also occur as dental pulp stones, some gall stones, salivary gland stones, chronic calculous prostatitis, testicular microliths, calcinosis cutis, several malignancies, calcific tendinitis, synovitis, arthritis, and cancerous tumors.^[1] In this section, we briefly discuss the calcification in tendons and breast cancer.

2.4.1. Calcific Tendonitis

Calcification in tendons, known as calcific tendonitis, is a rare condition that little is known about its mechanism hence limited effective therapies are available.^[67] It is defined by calcium crystal deposition (HAP) in tendons predominantly occurring in shoulder region with prevalence of 3% of adult population of age between 30 and 50 years old.^[68] In calcific tendonitis similarly to other pathologic calcifications such as in cardiovascular or renal systems, MVs are the main site of mineralization.^[67,69] The role of MVs is to provide enzymes required for regulation of extravascular internal tissue composition, which several studies showed that they contain necessary proteins for ion transport across membrane including annexin V^[70] and proteolipids.^[71] There are limited knowledge on the etiology of tendon calcification, recent studies have progressed on understanding the pathology of tendonitis.^[67] In the cases that symptoms are persisting, alternative treatments are investigating.

The treatment of symptomatic cases involves steroid injection^[72] or extracorporeal shockwave therapy (ESWT).^[73] However, recently, a more conservative therapeutical strategy using a combination of nonsteroidal anti-inflammatory drugs with physical therapy is suggesting as treatment approach.^[74] The effectiveness of these treatments decreases with severity of calcification^[73]; hence, more research is required to enhance

knowledge on the calcification mechanism to offer much efficient treatments.

2.4.2. Breast Cancer

The presence of calcified deposits in tumors is commonly reported, which 40% of breast cancer patients are presented with microcalcification (MC) in breast tissue and is diagnosed by mammography.^[75] Breast MCs are calcium mineral deposits in breast tissue that are an important screening tool for diagnosis of benign or malignant breast cancer.^[76] Studies showed the morphology of MC can be related to the aggressiveness of the tumor, for example, casting-type MCs are reported in aggressive tumor pathology compared to crushed stone (pleomorphic) or powdery.^[75,76] The overexpression of human epidermal growth factor receptor type 2 (HER-2) is highly associated with the occurrence of MCs in premalignant breast lesions, which can be an indicator of aggressive tumor growth.^[75,77] The relationship of MCs and breast cancer prognosis is not clear yet. The material characterization techniques have been of great importance in analyzing different types of MCs to expand the understanding on its connection with breast cancer process.^[78–80] Two major types of MCs are identified in breast tissue as type I deposits consist of calcium oxalate dihydrate and type II deposits contain calcium phosphates, mainly HAP.^[79,80] More detailed information is reported by Haka et al. in their Raman spectroscopy analysis on MCs in breast tissue.^[80] They showed type II MCs occur in benign lesions and contain lower levels of protein and higher calcium carbonate content.^[80] Similar to other pathological mineralization, mechanism pathway in breast cancer tissue leading to MC formation is unknown, and it is most likely involves complex interactions between extracellular and cellular components with mineral moieties. Investigating possible mechanisms of calcification in cardiovascular system, kidney and brain could lead us to a more universal mineralization pathway.

3. Mechanism of Calcification

Mineralization is a physical–chemical process and in biological systems is regulated by cells and their extracellular matrices.^[15] In chemistry, mineral deposition occurs when its solubility is surpassed. The classical nucleation theory (CNT) states that the crystal nucleates from elementary elements such as ions and molecules in a supersaturated solution, where this step is essential in crystal growth.^[81] In recent years, several theories have emerged in describing nucleation process, where CNT follows the Gibbsian concept of an energy barrier.^[82] The initiation of mineralization requires high activation energy to overcome the energy barrier and create the prenucleation cluster. However, this energy decreases by cells and vascular system providing high concentrations of ions for the formation of initial crystal.^[15,29] Recent findings suggesting that there is a multistage nucleation process in contrary to CNT that are known as nonclassical nucleation theories.^[82] In pathological and physiological calcification process, surface defects, dead cells, collagen fibrils, elastin, lipids, and bone regulatory proteins can decrease the energy barrier and act as nucleation sites leading to heterogenous calcification.^[29,82]

The spreading pattern of calcified deposits within tissues is affected by the flow of body fluid and the location of the calcification that is susceptible to shear and compressive stresses such as in valve openings and closings.^[29] Different morphologies of the calcified deposits within tissues have also been observed including, spherical particles, needle-like crystals, and small/large mineral aggregates.^[32] Thermodynamically unstable Ca-P goes through phase transformations to reach a stable crystals phase; hence, different morphologies occur during the calcification.^[32] In vivo and in vitro calcification models differ in their mineral deposition speed. The calcification process in vivo results from years of accumulation of minerals due to the presence of OPN and other regulatory factors (explained later in this section) within the natural tissue environment acting as inhibitors of calcification.^[29] On the contrary, the mineralization can occur only in a period of days in either elastin,^[13] collagen,^[14] or synthetic in vitro models.^[83] The rate of crystal formation and thermodynamics of mineralization is widely debated area that is discussed in recent review articles.^[81,82]

Evidence shows that the biomineralization process in soft tissues is a highly regulated contest between calcification promoters and inhibitory factors; however, the exact molecular mechanism controlling this process is not well understood.^[16,44,84] One method to understand the pathological calcification is to study the mechanism of mineralization in natural bone and teeth. It is evident from crystal formation in bone that the initial nucleation starts from MVs that contain free cholesterol, phospholipids, glycolipids, substantial quantities of phosphatidylserine and the calcium-binding proteins annexin II and V, and deposits of calcium and large quantities of alkaline phosphatase (ALP).^[85,86] Several studies have focused on analysis of proteins involving in kidney stone formation, in which a number of macromolecules, including OPN,^[87] matrix Gla protein (MGP),^[88] bikunin^[89] and Tamm-Horsfall proteins,^[90] are identified in urine and kidney stone samples (Figure 4A). However, close to 1000 proteins have been identified in an urinary proteome analysis that these proteins may play a vital role in crystal formation through interactions with each other.^[91]

Reviewed by Abedin et al., in atherosclerotic plaques and mineral formation, several factors are responsible in regulating the mineralization including bone morphogenetic protein-2 (BMP-2), OPN, osteoprotegerin, matrix-carboxyglutamic acid protein (MGP), and pyrophosphates, as well as smaller molecules such as carbonates and magnesium ions.^[92] On the other hand, the loss of mineralization inhibitory factors, such as MGP and extracellular inorganic pyrophosphate, is more evident in calcified tissues.^[93] In addition, it is also well known that there is potential for the osteogenic differentiation of a subpopulation of primary vascular smooth muscle cells (VSMCs) within cardiovascular tissues, where the mechanisms are not yet fully understood (Figure 4A).^[92]

The role of macromolecules such as GAGs in directing the mineralization is a highly acceptable fact in the bone; similarly, matrix–mineral interface relationship is evident in calcified plaques through a predominance of GAGs.^[94,95] In calcified lesions, the GAGs are intermixed with collagen fibrils, and as plaques develop, the GAGs accumulate within the ECM. Moreover, the negative effect of GAGs in calcified lesions is also their tendency to bind to low-density lipoproteins that retains cholesterol,

which create proinflammatory signals.^[37] Although mineralization-associated proteins are not highly evident in atherosclerotic mineral, but a clear protein–mineral interaction is yet unknown.

3.1. Matrix Vesicles

Extracellular membrane-bound structures known as MVs have been identified as a key factor in initiating the nucleation of HAP in physiological mineralization.^[85] The MVs originate from the plasma membrane of chondrocytes and osteoblasts.^[86] Being 100 to 700 nm-sized vesicles, the mineral formed by MVs has been observed in SEM images of aortic valve and media calcification and in atherosclerotic lesions.^[85] These vesicles contain HAP nanocrystals that are evident in early stage of mineralization. In contrast to spherical particles in aortic valve calcification, the MVs are smaller in size with only 100 nm in diameter.^[16] MVs are hollow in their core and contain amorphous minerals.^[16] In the analysis of calcification in the vessels, similar bone tissue biomineralization processes occur and MVs have been identified in both the tunica interna and media of the vessel wall.^[85] The formation of MVs is triggered by intercellular calcium signal that results in gene transcription.^[86] Although the mechanism behind the nucleation of HAP by MVs is not well understood, these vesicles are enriched in calcium-binding annexins (Anx) and surface ALP, which take part in inhibiting the activity of pyrophosphate (a HAP inhibitor factor).^[86] The role of MVs in vascular calcification has been studied by ultrastructural analysis; however, it is believed that VSMCs have a key role in regulating the mineralization process, by going through phenotypic change and expression of mineralization-regulating proteins.^[86] The mineralization inhibitors are the reason behind preventing calcification of VSMCs in a healthy tissue environment. The formation of MVs is observed in patients with atherosclerotic and CKD that were clustered with elastin and collagen fibrils but showed no evidence of mineralization in the ECM components.^[86] What is clear in MV formation is the elevation of extracellular calcium that triggers the VSMC response.^[86,96,97]

3.2. Cellular Factors in Calcification

The concept of cellular activities in calcification mechanisms has started to direct the researchers to the possibility of mineralization in VSMCs.^[92] Osteoclasts, large multinucleated cells, are the cellular part that absorb the minerals in natural bone. The actin ring around the osteoclasts provides a protease-rich, acidic microenvironment that is required for mineral absorption.^[92] Atherosclerotic lesions being rich in monocytes and macrophages, which the macrophages may contribute to vascular cell mineralization through promoting inflammatory cytokines and producing lipid oxidation products.^[92]

One technique that gives important information on formed biominerals is solid-state NMR that has shown similarities between the minerals in bone tissue and atherosclerotic plaques.^[37] Similar patterns have also been reported in the calcification of human aortic valve resembling natural bone structure that involves osteoblast-like cellular developments.^[30] Similar to bone, the cellular MVs have also been identified as the nucleation sites within the atherosclerotic plaques.^[86] The obvious

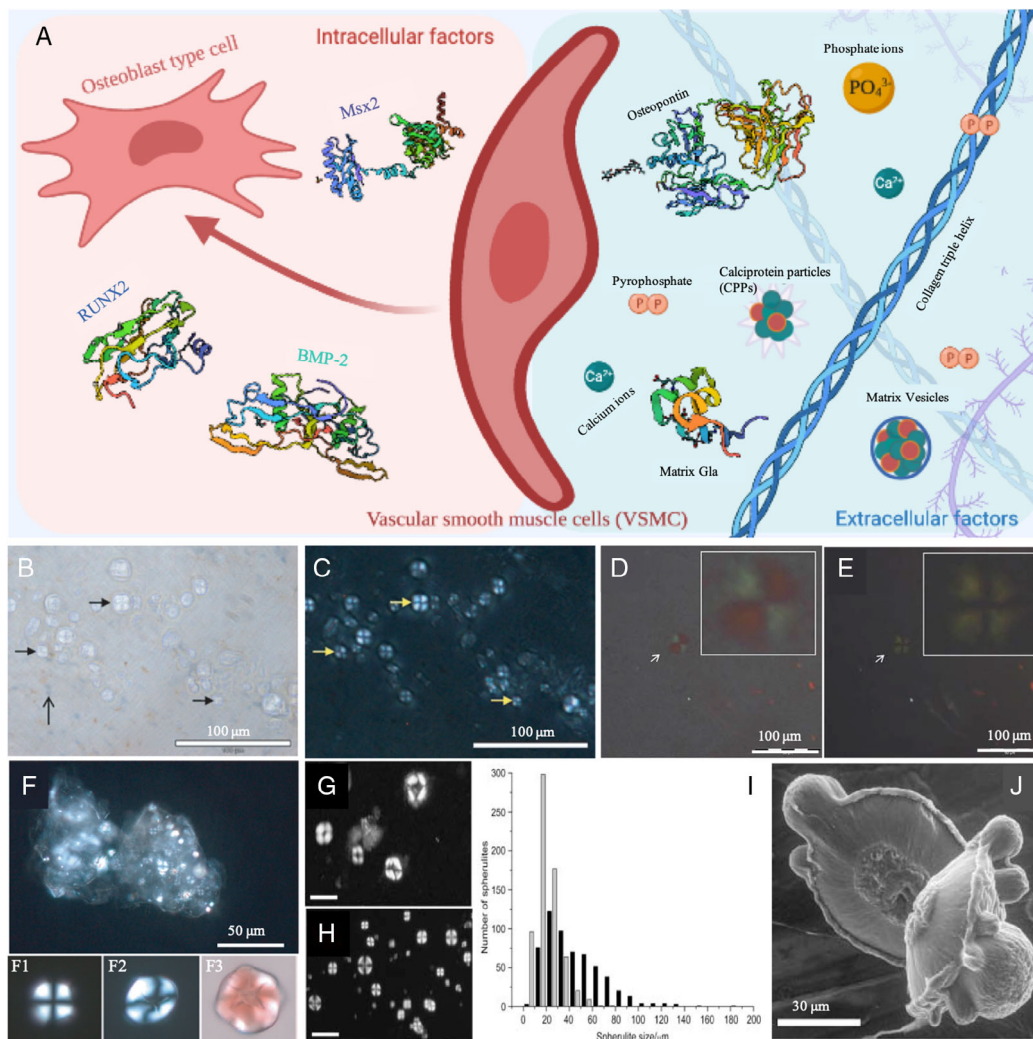


Figure 4. Schematic showing the cellular factors inducing the differentiation of VSMCs to osteoblast-type cells and the ECM molecules effects on calcification (A) (Created with BioRender.com); spherulites observed in AD hippocampal tissue stained with Congo red and haematoxylin and spherulites notably lack affinity for hematoxylin (solid arrow-heads) shown under partially crossed polarizers (B) and same region under fully crossed polarizers (C). Reproduced with permission.^[131] Copyright 2010, IOS Press, brain tissue section (20 μm thickness) from occipital lobe stained with modified hematoxylin and Highman's Congo red and showing (arrow and insert) a spherulite under partially polarized light (D) crossed polarizers (E). Reproduced with permission.^[163] Copyright 2011, IOS Press, large group of spherulites of A β 42 formed under near-physiological conditions in vitro (F) spherulite 10–12 μm in diameter with no core (F1), spherulite 15–20 μm in diameter with clear core (F2) spherulite 15–20 μm in diameter stained with Congo red (F3). Reproduced with permission.^[131] Copyright 2010, IOS Press, insulin amyloid spherulites formed without (G) and in the presence of NaCl (H), spherulite size distribution (I), and ESEM images of insulin spherulites (J). Reproduced with permission.^[130] Copyright 2005, Elsevier.

difference of pathological calcification with bone mineralization is that the HAp mineralization is well-organized and controlled process in natural bone formation, whereas the pathological calcification is rather uncontrolled.

3.2.1. Cell Phenotype

Cardiovascular calcification has been known for being a passive process, which is driven by high concentrations of calcium and phosphate ions within the tissues, leading to mineral deposition.^[98] However, studies have revealed the important role of cellular compartments in the mineralization process.^[98,99] To study

this factor, Watson et al. used oxysterol 25-hydroxycholesterol and transforming growth factor- β 1 (TGF- β 1), which are known factors in atherosclerotic lesions to stimulate the calcium–mineral nodule formation.^[99] Results confirmed the effect of 25-hydroxycholesterol in increasing the nodule formation compared to control.^[99]

The evidence including the presence of bone-related proteins and transcription factors in calcified deposits of atherosclerotic intimal and medial areas, signifying the role of cells in vascular wall.^[30] Apart from the lineage of the cells present in vascular walls, the transcription factors, such as Runx2/Cbfa1, Msx2, and osterix (SP7), direct the phenotype of cells phenotype toward

osteoblast lineages.^[30,98] Runx2 alone is a transcription factor that is enough to drive the differentiation of smooth muscle cells (SMCs) differentiation to an osteogenic lineage is Runx2.^[100] In vascular calcification, SMCs are the mostly studied cell population, where in vitro SMC-rich cultures in media containing osteogenic differentiation factors (β -glycerophosphate and l-ascorbic acid-2-phosphate) have demonstrated enhanced calcification.^[101] This process starts from apoptosis of SMCs and is followed by the release of extracellular vesicles (EVs) that are rich in tissue nonspecific alkaline phosphatase (TNAP) that act as nucleator sites.^[102] Moreover, identification of cellular contribution to calcification of aortic valve is rather challenging as the mineralization capacity of VICs is unknown.^[98] Some in vitro studies have shown the growth of calcific nodules by VICs in the presence of the cytokine-transforming growth factor- β 1 through apoptotic-dependent mechanism.^[103]

3.3. Osteogenic Factors

In the 19th century, pathological studies on atherosclerotic arteries revealed that the pathologic tissue resembles a bone-like lamellar structure with osteoblast-like cells and hematopoietic elements.^[92] The key regulators in the osteogenic process are also expressed in atherosclerotic plaques, including BMP-2,^[104] OPN,^[105] MGP,^[106] and osteoprotegerin (OPG).^[107] The factors that are identified in increasing the calcium build up in atherosclerotic plaques are modified lipid content, proinflammatory cytokines, phosphate, lipoprotein complexes, and foci of necrosis.^[38] Here, we look into the role of regulatory factors in soft tissue calcification that act as either inhibitors or promoters in osteogenic process.

3.3.1. Inhibitors

Matrix Gla Protein (MGP): MGP is a bone matrix protein that appears in atherosclerotic plaques and artery walls, in which the post-translational modification of its glutamic acid residues by carboxylation affects its function.^[108] While the role of MGP in mineralization is not well understood, studies have suggested that the MGP participates in homeostatic regulatory mechanism and limits the mineralization. Also, it has been suggested that MGP's role in regulating the mineralization is through control of the differentiation of mesenchymal stem cells to the osteogenic lineage by limiting production of BMP-2 thus preventing its interaction with receptors.^[109] The effect of MGP with BMP-2 highly depending on the carboxylation of MGP and concentrations of each molecule.^[110] The factor that controls the carboxylation of MGP is a vitamin K-dependent enzyme called carboxylase; therefore, deficiency of vitamin K may increase the rates of vascular calcification.^[110,111]

Osteopontin: OPN is a noncollagenous matrix protein that regulates mineralization in bone and dentine as connective tissues, but is also associated with calcifications in cardiovascular and renal systems.^[112] Looking into the polypeptide structure of OPN, high contents of negatively charged amino acids such as aspartate, glutamate, and serine are evident.^[113] The central section of the protein contains a highly negatively charged section that adopts α -helical structure.^[113] OPN has potential attachment

capability to different types of cells and its phosphorylated version regulates the anchorage-dependent growth and phenotype transformation in cells.^[113] The role of OPN in bone mineralization is thought to be on regulating the rate of crystal growth rather than nucleating the HAp mineral. It binds to the mineral surface via GRGDS segment and the aspartate-rich region.^[113] The inhibitory behavior of OPN during calcification is activated through the RGD motif that binds to cells via α -v and β -3 integrins.^[92] It has been shown by Giachelli et al. that OPN associates with calcified atherosclerotic plaques^[114] and has a role in preventing the growth of calcified crystals.^[92] Another inhibitory role of OPN may be through stimulating resorption via binding to osteoclasts, which results in decreased cytosolic calcium.^[115] This interaction of OPN with cells is dependent on the calcium concentration, which affects the conformation of the protein.^[113]

OPN has an essential role in inhibiting calcium oxalate growth and renal stone formation, and the pathway of inhibition is through preventing the COM growth. The COD growth is regulated by OPN, where more COD would incorporate more OSP molecules, which is a two-way interaction.^[116] COD crystals are more readily prone to clearance with urine and they have a lower tendency to adhere to cell surfaces.^[117] This can be the inhibitory mechanism role of OPN in HAp crystal growth. The phosphorylation of OPN increases its mineral-regulating effect.^[116] For example, McKee and co-workers have studied the incorporation of a serine and aspartate-rich motif, which is present in the family of Small Integrin-Binding Ligand N-linked Glycosylated proteins.^[116] They have shown that with an increase in negative charge and concentration of phosphorylated peptides, there was greater control on the crystal morphology and elongation via binding to COD, resulting in the formation of mushroom, dumbbell, and rosette-like crystals.^[116] The calcification mechanism of OPN is acellular and is a passive process, although the calcification is more a cellular-mediated process in bone and aortic valves.^[112] In the renal system, the epithelial cells showed different capacity for producing OPN mRNA depending on the age of the kidney, where younger kidneys were capable of upregulating the secretion of OPN, to suppress the calcium oxalate crystal growth.^[113]

Osteoprotegerin (OPG): OPG is a glycoprotein that regulates bone formation, as identified by Simonet as one of the tumor necrosis factor (TNF) receptor superfamily.^[118] OPG inhibits the later stages of osteoclast differentiation via the blocking of RANKL, which promotes calcification in cardiac valve myofibroblasts.^[119]

Fetuin-A and Calciprotein Particles (CPPs): Fetuin-A is another factor that plays an important role in controlling the clearance of calcium phosphate-protein complexes called calciprotein particles (CPPs).^[120] Being a glycoprotein – fetuin-A is a plasma protein that is abundant in CPPs and circulates the inhibitors of HAp.^[121] The inhibitory effect of fetuin-A is revealed through clinical data showing lower levels of fetuin-A in urine serum of patients suffering from calcification diseases.^[38,120] Studies on mice have shown that the fetuin-A deficiency, in addition to calcification-prone genetic factors, is the main reason leading to ectopic calcification.^[120] This can be avoided by the supplementation of calcification inhibitors including fetuin-A, pyrophosphate, and magnesium.^[120] The effect of fetuin-A in stabilizing the vesicle-mediating calcification is also evident in

SMC calcification.^[120] The concentration of serum fetuin-A in urine samples of dialysis patients is reported as a predictor of mortality leading to atherosclerosis.^[121] As reported by Bilgir et al.,^[122] lower fetuin-A levels have been detected in patients with stable angina and myocardial infarction. Due to the high risk of intimal and medial calcification in patients with CKD, monitoring the inhibitory factors could prevent vascular calcifications.^[121] The biological activity of CPPs is based on their crystallinity state, which at the ripening stage are only about 50–150 nm in diameter and are chemically unstable.^[120] Transformation of CPPs to larger size and stable state (up to 500 nm in length) is only possible in the presence of fetuin-A.^[120]

Small Molecules: Inorganic Pyrophosphate: Some ubiquitous small molecules act as mineralization inhibitors, for example, in a study by O'Neil et al., it was shown that the administration of pyrophosphate reduces the ectopic calcification of blood vessels.^[123] The ratio of phosphate–pyrophosphate is an important factor in the development of vascular mineralization.^[123] This finding can render the pyrophosphates as promising treatment for CKD patients.^[124] The process of pyrophosphate transformation to phosphate ions is controlled by the transporter ANK exporting through the plasma membrane, which is then degraded by TNAP.^[124] The constant removal of inhibitory pyrophosphate and generation of two orthophosphate ions favor the mineralization in tissues. In using the pyrophosphate as a treatment, the short half-life of this molecule should be taken into consideration as it has a half-life of 30 min in rats.^[124]

Bisphosphonates: As alternative nonhydrolyzable analogs of pyrophosphate, bisphosphonates have been used in the treatment of osteoporosis in low doses, while at higher doses of bisphosphonates have been shown to prevent vascular calcification.^[124] However, higher dosages of bisphosphonates have adverse effects on skeletal biology and most of the nephrologists would refrain from prescribing bisphosphonates for their CKD patients.^[124]

Magnesium: The effect of magnesium ions (Mg^{2+}) on the formation of calcified tissues can be explained through the formation process of apatite precursors such as amorphous calcium phosphate, dicalcium phosphate dihydrate, and octacalcium phosphate.^[125] Mg^{2+} ions tend to delay the rate of HAp crystallization, and this process can be explained by the blocking of mineralization sites on the crystal surfaces by magnesium ions.^[125]

However, increased magnesium and acidic environment can direct the whitlockite formation over HA, which in kidney whitlockite formation is unaffected by Mg^{2+} levels in the environment.^[126] It can be said that the local Mg^{2+} concentration determines the type of the formed mineral.

3.3.2. Promoters

Cadherin-11: Cadherin-11 (Cad-11) is considered as one of the calcification promoter factors.^[26] Cad-11 is a cell–cell adhesion protein that plays a role in the differentiation of mesenchymal cells to osteo- and chondrogenic lineages.^[26] The expression of Cad-11 is important in preventing inflammation and degradation in cartilage, rheumatoid arthritis, and multiple cancer types.^[26] On the other hand, increased levels of Cad-11 expression have been shown to promote inflammation and osteogenic

differentiation.^[127] Sung et al. showed that the calcification of valvular myofibroblasts through the cell–cell tension and aggregation of cells can be promoted by Cad-11.^[26] The signaling pathways mediated by RhoA^[26] control the Cad-11 expression, which leads to increased stress fiber bundle, compaction and collective migration, and results in calcific nodule formation.^[26]

Fibulin-7: Fibulin-7 (Fbln7), which is a matricellular protein and is structurally similar to elastogenic short fibulins, is another promoter factor.^[128] This protein has the tendency to bind to dental mesenchymal cells and heparin and has been detected in renal tubular epithelium and kidney that regulates the renal calcification.^[128] The expression of Fbln7 is induced by exogenous heparin due to the N-terminal domain of Fbln7 that binds to heparin through its coiled-coil domain.^[128] The role of Fbln7 in calcification is reported in Fbln7 knockout mice showing no evidence of calcification. A recent study by Tsunezumi et al. showed that Fbln7 can take part in renal tubules calcification by directing the CPP formation in pericellular matrix using the heparin-binding domain.^[128] The Fbln7 alleviates fibrosis and induces calcium phosphate deposition, but the Fbln7 acts locally in calcium phosphate crystallization and the mechanism behind this deposition is not known.^[128]

3.4. Protein Regulation of Mineralization

Throughout the mineralization process, proteins can act as epitaxial nucleators, as well as coatings of the mineral surface, to control the shape and size of the minerals. This process has been studied through the binding of HAp to proteins and peptides.^[15] Mineralized tissues utilizes proteins to provide a template for atomic-level molecular modeling.^[15] In physiological calcification of bone and enamel, it is evident that collagen and self-assembled matrix of amelogenin nanospheres template the nucleation and hence regulate the mineralization process, respectively.^[98,129] The fact that the majority of proteins involved in biomineralization and HAp formation are IDPs suggests that protein disorder plays a fundamental role in the formation of protein spherulites,^[12,130,131] amyloids,^[132,133] and calcification.^[133]

Looking into other neurodegenerative diseases such as AD, the spherulitic protein structures are evident with close relations to amyloid fibrils (Figure 4).^[131] Although several amyloidogenic proteins showed spherulite structures in vitro, such as amyloid- β in AD, α -synuclein in Parkinson's disease, and amylin in diabetes, but they have not been reported to form these structures in vivo.

The formation of spherulites in vivo is reported for A β 42, an amyloidogenic peptide that is found in the core of senile plaques in AD.^[131] A study by Exley et al. showed a similar Maltese cross pattern of amyloid spherulites in AD brain tissue with Congo red and hematoxylin staining^[131] (Figure 4F, F1–F3) that can be visualized under polarized microscopy due to their birefringence property.^[134] The relation of these spherulite structures to AD is still unknown, but the disordered proteins and their mineralization can be used to shed some light on amyloid structures. A few of amyloidogenic proteins including insulin, β -lactoglobulin, and albumin have been shown to form spherulites under physiological conditions in vitro (Figure 4G–J).^[131]

4. In vitro Models for Pathological Calcification

The successful design of scaffolds or in vitro models would benefit the field in terms of understanding the calcification mechanisms, by studying the interaction of minerals with the ECM components and closely monitoring the crystal nucleation process.^[12] Understanding the rules that dictate the development of calcified lesions across multiple tissues, while expanding from nano- to macro- scales, is an ultimate but yet unattained goal. Inspired by nature, natural molecules such as peptides and proteins have been used in developing models for studying calcification processes.^[12,13] Toward this goal, protein's building blocks, amino acids with negatively charged side chains, have been used in the design of scaffolds^[135] or in the self-assembly of polymeric hydrogels.^[136] Synthetic mineralization platforms that can emulate the features of these dynamic supramolecular matrices, exhibiting disorder–order optimization, may lead to the design of materials capable of recreating the structure and properties of pathological calcified tissues, as well as study their mechanisms of formation. The generation of these in vitro models will represent a critical leap not only to elucidate the mechanisms of pathological calcifications but also to provide strategies to tackle these disorders.

4.1. Polymers

Inspired by nature, several templates have been developed for creating biomaterials with complex and sophisticated structures mimicking their biological counterparts.^[137] With the aim of fabricating biomaterials with mineralization ability, natural building blocks including peptides, proteins, polysaccharides, and lipids are incorporated as nucleation sites, promoters, or inhibitors of crystallization.^[137] However, the use of synthetic polymers has gained importance in biomaterials research due to their high strength and stiffness in addition to their simple synthesis.^[137] As an example of simple synthesis, homogeneous aragonite crystals are shown to form on particles of a hydrophilic triblock copolymer, poly(diethylaminoethyl methacrylate)-*b*-poly(*N* isopropylacrylamide)-*b*-poly(methacrylic acid) (PDEAEMA-*b*-PNIPAM-*b*-PMAA), which can be synthesized in an ambient environment and using aqueous conditions following a standard vapor diffusion method (Figure 5).^[138] In mineralization of polymers, using “double hydrophilic block copolymers” can mimic the natural mineralization in biological systems, in which the polyelectrolyte block interacts with crystal surfaces and the other nonionic block provides the water solubility.^[138] Due to their superior mechanical properties, synthetic polymers have been used in the design of aortic valves. However, these polymeric valves are prone to calcification especially on the blood-containing polymer membrane surface.^[139] Membranes fabricated from polyurethanes and their copolymers were the first generation of polymeric heart valves, which showed high rates of calcification under fatigue tests.^[140] Polyurethane valves failed in two main ways; first, by developing holes in the central leaflet area and second by tearing on the sides of the leaflet.^[140]

Other polymers, such as polycarbonate (PCU) and polyhedral oligomeric silsesquioxanes (POSS) nanocomposites, have also been developed as replacement candidates for synthetic heart

valve leaflet application.^[141] The POSS-PCU nanocomposite has shown higher tensile strength compared to polyurethane-based elastomers such as Estane®, Chronoflex C®, and Elasteon™ (Figure 5C).^[141] Despite the excellent mechanical properties, there is a lack of long-term studies to prove the compatibility and calcification resistance of these nanocomposite synthetic valve materials.^[141] In fact, the main drawback of synthetic polymer models is their lack of biocompatibility, which directed research toward natural polymers in developing in vitro models.

4.2. Collagen Models

Three dimensional scaffold models are great alternatives to study the biomechanics and changes occurring in healthy and diseased tissues, in vitro. In designing biomaterials for mimicking the native tissue ECM, several factors should be considered such as, biocompatibility, cost, amenability to sterilization techniques and easy handling. Several nature-inspired biomaterials are designed to mimic the native mineralization processes of tissues (Figure 5 second section).

Collagen type I, as one of the main fibrillar component in bone ECM, has been used in the design of three-dimensional models for mimicking bone structure.^[14] In engineering a model for arterial calcification, collagen hydrogels have been exploited to mimic the chemical and mechanical changes of the healthy tissue through mineralization process.^[142] Farrar et al. reported an inexpensive and versatile technique for manufacturing collagen hydrogels to mimic the aortic valve tissue.^[143] This system is compatible with live-imaging techniques, and each section of the hydrogel can be sectioned and treated for characterization accordingly. The microenvironment mechanical and chemical properties strongly affect the cellular behavior in the native tissue. For example, the biomechanics of native aortic valve tissue is tested by designing collagen hydrogels with controlled tension.^[143] The formation of calcific nodules hardens the ECM of native tissue in aortic valves and changes the VICs phenotype that is affected by the mechanical signaling from the ECM (Figure 6A).^[143] The changes in the ECM composition influence the VIC phenotype, on the other hand, the changes in VIC's homeostasis result in a complex cellular feedback loop that changes the extracellular environment.^[143] Early in their studies, the increase in TGF-β1 activity of VICs is correlated with the ascorbic acid, and *b*-glycerophosphate in the osteogenic media that also induces ALP expression in osteoblastic differentiation.^[143] The calcification process affects the ECM arrangement of VICs, disrupting the cell and collagen fiber alignment (Figure 6B).^[143]

Another advantage of using biomaterials as models for creating the calcification is to be able to closely follow the mineral growth. As an example, the effect of collagen on mineral growth was studied by Wang et al. revealing that the collagen fibers are enough to initiate and orientate the growth of CHA without the assistance of any other ECM molecules.^[144] The role of EVs in directing the vascular calcification is as yet unknown. Hutcheson et al. developed an in vitro model of collagen-I hydrogel to directly observe the calcification process and contribution of EVs to the formation of atherosclerotic plaques.^[98] Their process incubated collagen hydrogels in media containing EVs that were collected from cultures of SMCs.^[98] The formation of EVs after three days exhibited a dense calcifying structures

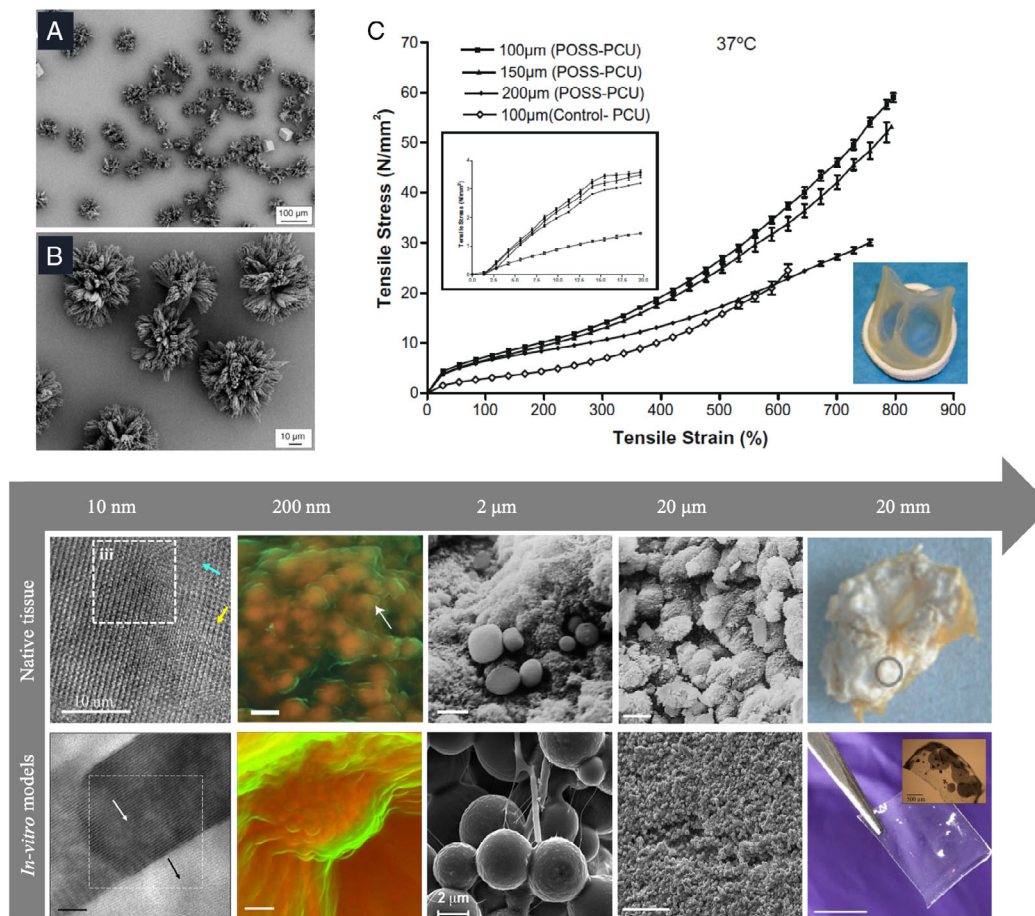


Figure 5. Higher (A) and lower (B) magnification SEM images of “sheaf bundle” crystals of hydrophilic block copolymer. Reproduced with permission.^[138] Copyright 2005, John Wiley and Sons, stress–strain curves of POSS-PCU nanocomposite heart valve at 37 °C (C). Reproduced with permission.^[141] Copyright 2009, Elsevier. Bottom section: Transference of pathological calcification to in vitro models: Top: structural characterization of calcified cardiovascular tissue. From left to right: high-resolution transmission electron micrographs (HRTEM) of whitlockite particle from human aorta tissue. Reproduced with permission.^[52] Copyright 2017, Imperial College London, DDC-SEM of a large calcification within a human carotid artery plaque. Reproduced with permission.^[98] Copyright 2016, Springer Nature, SEM micrographs of aortic calcified deposits (higher magnification – 4 μm) and (lower magnification – 20 μm). Reproduced with permission.^[5] Copyright 2001, Springer Nature, and calcified deposits in human aortic valve. Reproduced with permission.^[2] Copyright 2013, Springer Nature. Bottom row: structural characterization of in vitro models for calcification. From left to right: FIB sectioning of the hierarchically mineralized structure of elastin-like recombinamers (ELR) membrane’s mineralized core (10 nm). Reproduced with permission.^[12] Copyright 2018, Springer Nature, deeper within the bulk of the ELR membrane (200 nm). Reproduced with permission.^[12] Copyright 2018, Springer Nature. SEM images of elastin-like protein (ELP) membranes. Reproduced with permission.^[13] Copyright 2019, American Chemical Society.), calcium phosphate minerals covering the peptide amphiphile/PSS hydrogel fibers (20 μm). Reproduced with permission.^[83] Copyright 2019, American Chemical Society, and mineralized ELR membrane (5 cm). Reproduced with permission.^[12] Copyright 2018, Springer Nature.

(Figure 6C–E) resembling calcified human plaques, where their sizes depended on changes in collagen concentration.^[98] Another example of an in vitro model of a collagen-I hydrogel to evaluate the importance of the microenvironment, such as gel density and anisotropy on the functionality of cells, was evaluated by Griffanti et al.^[145] An ad hoc 3D bioprinter was used to fabricate VSMC-seeded tubular collagen bio-inks characterized by well-defined fibrillar density and anisotropy. Interestingly, VSMCs displayed a functional contractile state when seeded in less dense bio-inks characterized by a randomly oriented fibrillar architecture, whereas they did not display a contractile state when seeded in more compact bio-inks with an anisotropic fibrillar architecture.^[145] This suggested that VSMC functionality can be

controlled through matrix density and architecture and may represent an interesting alternative for the study of pathological mechanisms. In another study, the effect of HAP’s crystallinity is examined using collagen hydrogels to mimic the human diseased heart valves.^[146] The severity of the disease can be correlated with carbonated content and crystallinity of minerals.^[146] By varying HAP crystallinity, cellular response to mineral-rich environment is studied by Richards et al. following a simple set up of collagen hydrogels (Figure 6F).^[146] The concentration and crystallinity of HAP particles had a direct effect on the formation of larger aggregates (Figure 6G,H), which through controlling the concentration of incorporated HAP, different diseases severity can be imitated.^[146]

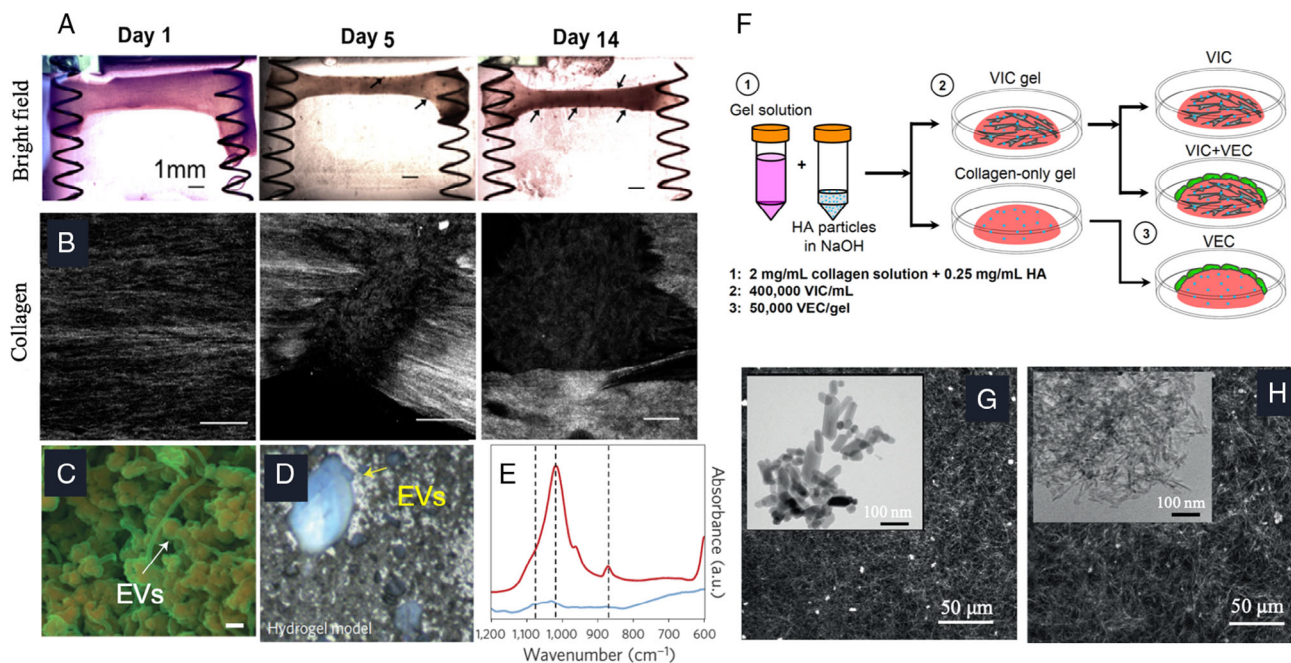


Figure 6. Mechanically active VIC hydrogels showing nodules: bright field images of hydrogels at days 1, 5, and 14 (A, arrows indicate nodules), immunofluorescence of hydrogels revealing collagen fibres in white (B). Reproduced with permission.^[143] Copyright 2016, Elsevier. DDC-SEM of calcifying EVs within a synthetic collagen hydrogel (scale bars, 500 nm) (C), bright field image of collagen hydrogel indicating EVs (yellow arrow) (D), FTIR absorbance spectra of large calcification (dark red spectrum line) and microcalcification (light blue spectrum line) (E). Reproduced with permission.^[98] Copyright 2019, Springer Nature. Schematic preparing HAp-containing collagen hydrogels (F), incorporation of poorly crystalline HAp1 (G) and crystalline HAp2 (H) particles inside the collagen hydrogels (0.25 mg ml⁻¹, insert is TEM image of HAp particles). Reproduced with permission.^[146] Copyright 2018, Elsevier.

4.3. Elastin Models

In arterial calcification, the ECM proteins influence where the calcification occurs being either intimal or medial calcification. For instance, intimal calcification is mostly deposited on collagen fibers, whereas medial calcification targets the elastin as the main mineral nucleator.^[13] One approach to better comprehend the cardiovascular calcification mechanism is using elastin as a model molecule.^[13] Elastin is reported to provide a nucleating matrix that leads to calcification, as the solubilized elastin is shown by Starcher and Urry as a potential matrix candidate for in vitro calcification.^[147] Cross-linking of elastin-like peptides created a platform to study the mineralization patterns in different media including simulated body fluid (SBF)^[13] and HAp^[12] solutions. For example, Gourgas et al. utilized cross-linked elastin-like peptides to develop a model for medial arterial calcification.^[13] They used genipin to cross-link the elastin and form membranes, which showed a mineralization pattern similar to medial calcification when incubated in SBF (Figure 7A). The calcification starts by binding of calcium and mostly occurs on elastin fibers, showing the vulnerability of the fibers to mineralization.^[13]

The in vitro model of elastin membranes acted in a similar fashion to in vivo calcification of medial valve including the occurrence of thin flake minerals of HAp in radial arrangements after 28 days (Figure 7B,C) and 32 days of incubation (Figure 7D).^[13] The mineralized membranes showed similar diffraction rings to what has been reported for native bone corresponding to poorly crystalline HAp (Figure 7E,F).^[13]

Moreover, these models can be a good candidate to study the mechanical behavior of calcified tissues, as Gourgas et al. showed that the mineralized membranes lost their initial elasticity and get stiffer as it happens in medial calcification.^[13] This change in mechanical characterization of tissues leads to increased systolic and pulse pressure known as source of left ventricular hypertrophy and failure, aneurysm formation, and rupture.^[13] Looking from the physicochemical and compositional side to the mineralization of ELP₃ membranes, they showed the presence of HAp and CHA that are most abundant mineral phases in pathological calcification due to its thermodynamic stability.^[13] These membranes showed very small amount of OCP minerals that only picked up by Ca K-Edge near edge X-ray absorption fine structure spectroscopy (NEXAFS).^[13]

Similarly, Mata's group revealed that the interplay between disorder (random coils) to order (β -sheets/ α -helices) domains within IDPs is critical during mineralization (Figure 7G).^[12,13] The contribution of IDPs in the intermolecular interaction at the protein–mineral interface has been shown in amelogenin while interacting with enamel crystals^[11] as an example. The changes from disordered to ordered conformations are believed to be the source for mineral nucleation and growth.

Developing in vitro models that can create the optimizable disorder–order interplaying system is a promising approach in understanding the diseased environment. The elastin-like recombinamers (ELRs) have been used as a model recombinant macromolecule, due to their biocompatibility, biodegradability, and the presence of charged amino acids, to study the

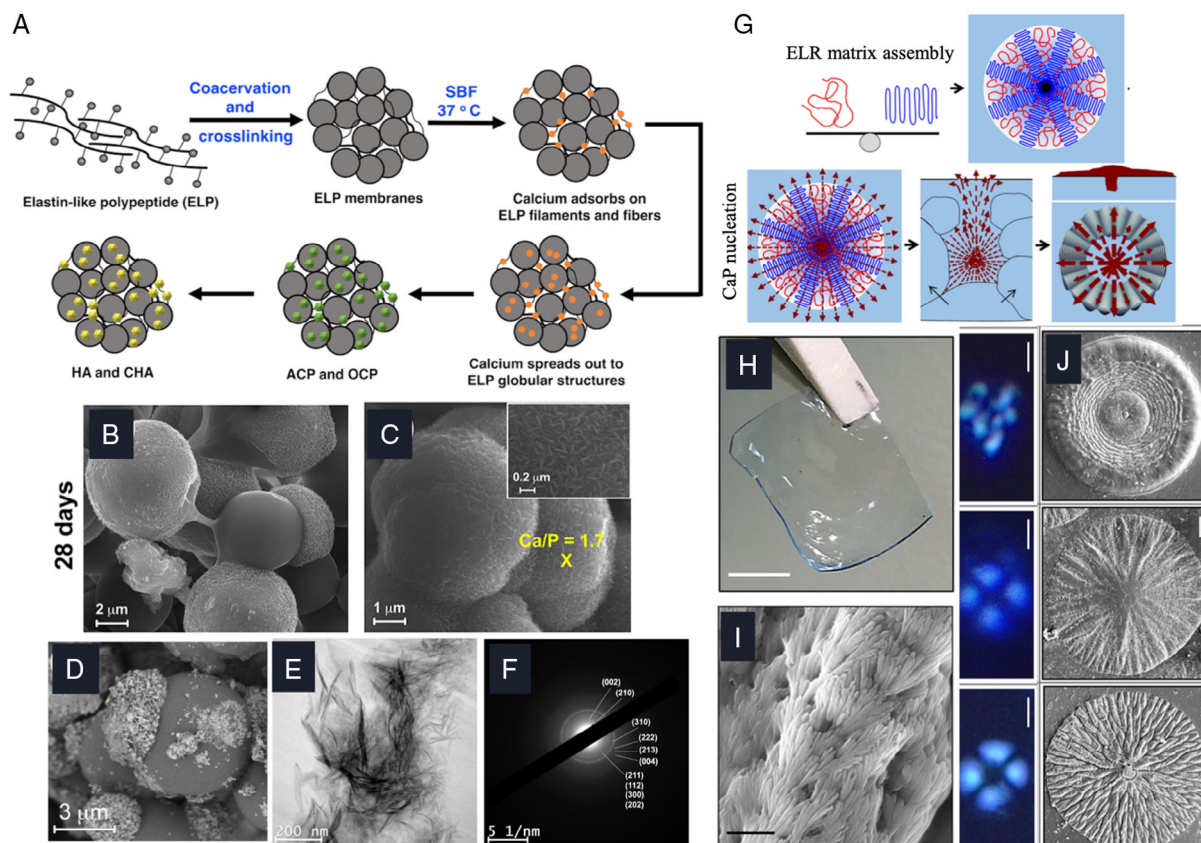


Figure 7. Schematic of mineralization mechanism (A), SEM images of ELP₃ membranes after incubation in SBF for 24 days (B,C) and 32 days (D), high-resolution TEM image of an ultrathin section ELP₃ membranes after 32 days incubation (E), SAED image from mineral region (F). Reproduced with permission.^[13] Copyright 2019, American Chemical Society. Schematic of ELR matrix assembly and nucleation (G), photograph of a transparent, robust, and flexible statherin-ELR membrane before mineralization (H), aligned fluorapatite nanocrystals (I), protein disorder–order optimization (Scale bars: 3 μm (ELR spherulite morphology), 20 μm (apatite hierarchical structures) (J). Reproduced with permission.^[12] Copyright 2018, Springer Nature.

mineralization process. The repeating unit of Val-Pro-Gly-X-Gly (VPGXG), where X can be any amino acid except proline, is similar to natural elastin and allows for it to be used as a model for IDP.^[148] In the designed ELR model by Elsharkawy et al., a hydrophobic segment of VPGIG and a positively charged segment as VPGKG were used that the lysine is the target site for cross-linking.^[12] The cross-linked membranes (Figure 7H) mineralized in highly saturated solution that resulted in spherulite-like hierarchical structures that grow radially into circular pattern (Figure 7I). The mineralization pattern not only covers the surface but also is evident within the membrane.^[12] The mineral type was confirmed by XRD data and ¹⁹F NMR, which are in agreement with fluorapatite crystalline phase. Further analysis into the crystallographic orientation of the mineralized membranes performed by HRTEM on super thin sections of the membrane (sectioned by FIB). The thin sections revealed a flat geometry at the end of their c-axis evidencing the effect of ELR matrix on interacting with fluorapatite crystals and providing an environment in favor of mineral growth.^[12] These membranes can be optimized through their disorder–order ratio by controlling the cross-linking agent that the spherulite formation and mineralization patterns depend on this ratio (Figure 7J).^[12] Incorporation of IDPs in the design of in vitro models can

provide us with insights into the mechanism of calcification in soft tissues such as cardio or brain that leads to severe diseases.^[12]

4.4. Other Models

Biomaterial approach as in vitro models has designed mostly targeting vascular system. Here, we discuss in vitro models for studying MVs in tendon calcification, mimicking kidney stones and investigating breast cancer MCs.

To study the interaction of ECM components and MVs, Gohr et al. designed an in vitro model using isolated MVs from adult porcine patellar tendons embedded in agarose gels and investigate the effect of ECM components such as type I collagen and dermatan sulfate on the mineralization of MVs.^[67] They showed the effect of dermatan sulfate, a major proteoglycan in tendon ECM, in suppressing the mineralization of tendon matrix vesicle, which changes such as aging and diabetes can cause interruption in ECM components' behavior leading to calcification of soft tissue.^[67] In another study, gelatin gels are used as in vitro model to study the mineralization mechanism of MVs isolated from chondrocytes culture.^[149] They indicated that changes in mineralization inhibitor such as enzymes, including adenosine triphosphate or ECM component, proteoglycans contribute to

lowering the calcification of MVs.^[149] The in vitro models used in this study, gelatin, is a denatured type I collagen that can downgrade the ionic concentrations compared to in vivo conditions.^[149]

In vitro models for studying the calcification in kidney are only limited to artificial kidney stones. These models are created to determine the effectiveness of various testing extract or compounds for treatment of urolithiasis.^[150] The benefits of in vitro models not only include preliminary studies before invasive in vivo testing but also prevent high number of costly replicates and animal studies.^[150] Conventional 2D cell culture models are used to inhibit the crystal-binding sites in renal epithelial cells that resulted in decreased crystal aggregation.^[150] However, 2D models are not representative of more complex in vivo conditions and does not incorporate ECM, inhibitors, and promoters of calcification. Despite the limitations of in vitro urolithiasis models, they can still provide great knowledge on prophylactic management to prevent stone recurrence and test effective laser treatments.^[151] One of the in vitro models used for mimicking the kidney stone formation is simultaneous flow static model (S.S.M.) that use salt-forming solution that dropwise is being collected in hot water then goes through crystallization by cooling and drying.^[150] Another model, silica-hydro gel acts as a growth medium, which seeding solution added to the formed gel reacts with the gel structure leading to the growth of different types of single urinary crystals.^[150] This model is used to evaluate the crystallization of urinary crystals.

The materials science has got close to study kidney stones in the field of artificial kidney stones that are useful in investigating the connection between laser parameters and stone fragmentation

patterns (Figure 8).^[151] Polymer-mineral composites and commonly used BegoStone, a dry gypsum plaster, are examples of artificial stones that seek to mimic the mechanical properties of human kidney stones.^[151] These artificial stones are used for extracorporeal shockwave lithotripsy research to better optimize the holmium laser lithotripsy treatments.^[151] The composite stones are made from COM as the primary mineral component of human kidney stone, uric acid, magnesium ammonium phosphate hexahydrate in an organic polymeric substrate (poly(ethylene-o-vinyl acetate)) (Figure 8B(insert) and C).^[151] Even though the microstructure of these artificial stones does not represent the human kidney stones, they share similar physical and spectroscopic properties that can be useful in single-pulse laser lithotripsy experiments.^[151] These in vitro models help to elucidate the response of kidney stones to laser treatments, but still there is a big gap in understating the mechanism of kidney stone formation. There is a great need for developing biomaterials to create a platform to study the mineral formation with consideration of more complex in vivo environment as an attempt to design better technologies in kidney stone management and prevention.

To understand the connection of malignancy of breast cancer and MCs mineral characteristics, in vitro models have been applied.^[76] Moreover, tissue-engineered scaffolds are used as in vitro platform to study the effect of HAp particle size on mammary cancer cell activity.^[152] The mineral-containing poly(lactide-co-glycolide) (PLG) scaffold showed that the particle size of HAp crystals modulates protein adsorption.^[152] Breast cancer cell growth and secretion of tumorigenic interleukin-8 (IL-8) are reported to change with HAp mineral morphology

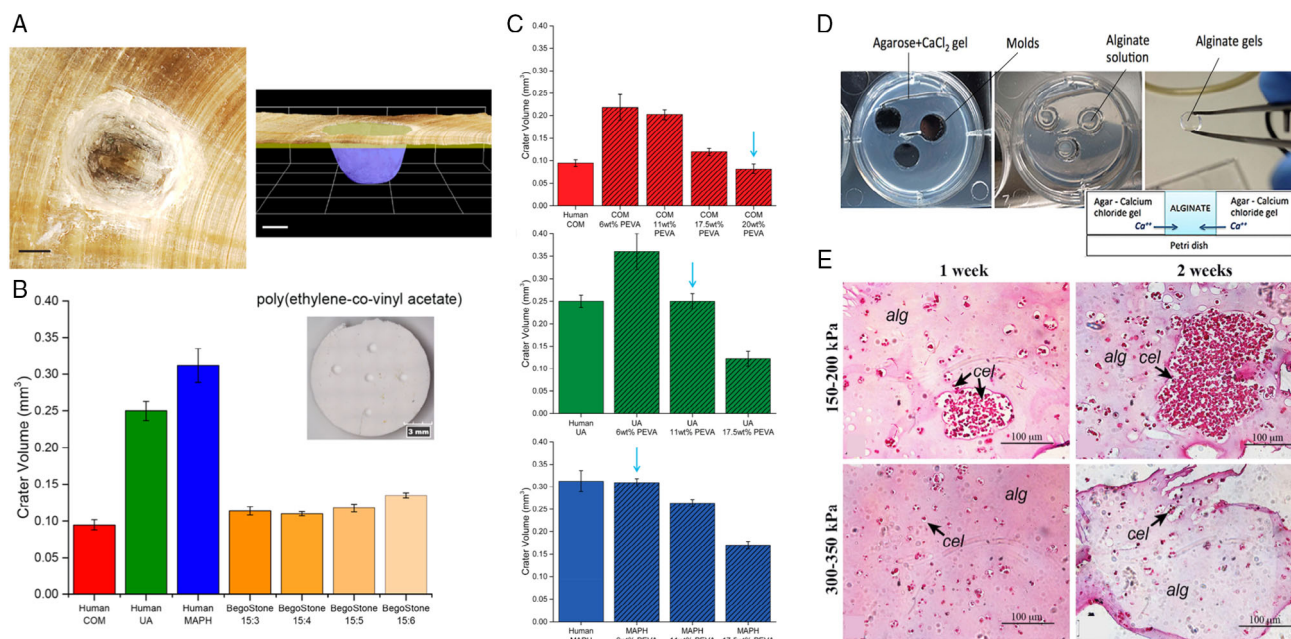


Figure 8. Other in vitro models: a crater formed from single-pulse holmium:YAG laser lithography experiment in a human COM stone (scale bar 150 μ m), multifocus image is shown on the left, and 3D reconstruction image is shown on the right (A), crater volume compared for human kidney stones and four types of BegoStone model with decreasing ratios of mineral to water (insert showing the mechanically robust artificial kidney stone PVA composite) (B) and crater volume graphs of composite artificial kidney stone models (red: COM mineral, green: UA mineral and blue: MAPH mineral) that the optimal concentration of the polymer is indicated by blue arrow (C). Reproduced with permission.^[151] Copyright 2019, American Chemical Society; alginate gel manufacturing process as summarized in (D) and cell proliferation and cluster formation are higher in softer gels reaching clusters of 100 μ m in one week (E). Reproduced with permission.^[156] Copyright 2016, Springer Nature.

and level of carbonate in the crystal, studied in a 2D mineralized culture plate.^[153] 2D in vitro models were also incorporated by Morgan group to study the calcium deposition and ALP activity of breast cancer cell lines with a combination of mineralizing reagents.^[154] Even though 2D culture models are suitable to investigate the effect of a factor or reagent on cell behavior, they have limitations in mimicking the 3D tissue microenvironment. Development of 3D microfluidic systems offer a 3D environment with properties similar to in vivo conditions specified for an organ.^[155] Cancer metastases are simulated in a 3D tri-culture microfluidic in vitro model with creating an osteo-cell microenvironment using collagen type I hydrogel.^[155] The mechanical support of ECM is an important parameter to include in the design of in vitro models. This has been applied in 3D alginate hydrogels that are mechanically tuned (Figure 8).^[156] The stiffness of alginate hydrogels is controlled by the crosslinker CaCl₂ content.^[156] The elastic modulus (E) of hydrogels was measured by atomic force microscopy and the effect of the elasticity of the microenvironment on breast adenocarcinoma cell activity.^[156] The stiffness of the gel affected the proliferation and cluster formation of cells that they form nigger clusters in softer gels (Figure 8E).^[156]

Several studies covered the required parameters in tissue-engineered scaffolds for mimicking bone structure.^[157,158] The essential properties including biocompatibility, porosity, surface properties, mechanical properties, and biodegradability^[157] are some of these parameters that most of these factors are also important in designing in vitro models for studying pathological calcification. However, the important factor to be considered for in vitro models is the ability to support mineral growth. Porosity and diffusion are essential for crystal nucleation and growth.^[158] Different strategies are reported to mimic biomineralization systems including premineralized scaffolds using SBF or HAp solution.^[12] Although in vitro models are not as extensively studied for pathological calcification as it has been for bone mineralization, but there is a great potential in developing a platform for studying pathological calcification in vitro. For this purpose, materials that are inspired from nature can be suitable candidates including mineralizing peptides^[159] and proteins.^[158]

5. Conclusion and Future Prospective

Pathological calcification is a complicated process that concerns several soft tissues including cardiovascular, brain, and renal systems. The exact mechanism that causes the deposition of minerals is not fully understood. However, the structural characterizations using high-resolution electron microscopy, XRD, and spectroscopy techniques provide us with information regarding the kinetics of mineralization, type, and morphology of minerals. The structure–function relationship of bone and teeth has been widely studied and using that as a reference would assist us in predicting the mechanism of pathological calcification.

Cardiovascular system being vulnerable tissue for calcification gives us a chance to study the microstructure of calcified deposits using advanced microscopy and spectroscopy techniques. The morphology of calcified deposits can be as spherical particles, fibrillar, or compact surface. Moreover, the two types of dystrophic and osteogenic calcification lead us to look into the effect of osteogenic factors and extracellular molecules on promoting the

calcification of soft tissues. On the other hand, the physicochemical analysis of minerals being either HAp, whitlockite, or other phases can help us in understanding the mechanism.

The mechanism of physiological calcification has demonstrated a balance between inhibitory and promoter factors in tissues such as bone. Osteogenic process takes place by the controlled imbalance between these two factors leading to the formation of MVs as precursors of bone minerals. Nevertheless, there are other components affecting the mineralization process being either intracellular or extracellular.

The ECM proteins such as collagen evidently act as a template for nucleation of bone minerals, and amelogenin acts as a template for growth of enamel nanospheres.^[98,129] Protein disorder and order assemblies play an important role in mineralization as most of the proteins involved in calcification are from the IDP family group. This fact can be confirmed by the formation of protein spherulites,^[12,130,131] amyloids,^[132,133] and calcification.^[133] Studying pathological calcification from the protein disorder point of view can be beneficial in predicting the mechanism through in vitro models such as designs studied with elastin membranes^[12,13] and collagen hydrogels.^[144] These models offer an opportunity to create the tissue-mimetic environment to simulate the pathological calcification to shine light on its mechanism of calcification. This approach would highly benefit the areas of pathological calcification such as brain calcification that lack the in vitro models to assist us in understanding the mechanism of mineralization. Clearly, further studies are required to advance more complex in vitro models that incorporate IDPs and cellular factors to eventually develop therapies and treatments for diseases caused by pathological calcification.

Acknowledgements

The authors would like to acknowledge the funding from Wellcome Trust, National Institute of Health Research, and King's Together Fund. The Table of Contents image is created with BioRender.com.

Conflict of Interest

The authors declare no conflict of interest.

Keywords

calcified deposits, in vitro models, intrinsically disordered proteins, pathological calcification

Received: March 25, 2021

Revised: May 9, 2021

Published online: July 3, 2021

- [1] N. Çiftçioğlu, D. S. McKay, *Pediatr. Res.* **2010**, *67*, 490.
- [2] S. Bertazzo, E. Gentleman, K. L. Cloyd, A. H. Chester, M. H. Yacoub, M. M. Stevens, *Nat. Mater.* **2013**, *12*, 576.
- [3] M. Nichols, N. Townsend, P. Scarborough, M. Rayner, *Eur. Heart J.* **2013**, *34*, 3028.
- [4] A. Timmis, N. Townsend, C. P. Gale, A. Torbica, M. Lettino, S. E. Petersen, E. A. Mossialos, A. P. Maggioni, D. Kazakiewicz, H. T. May, *Eur. Heart J.* **2020**, *41*, 12.

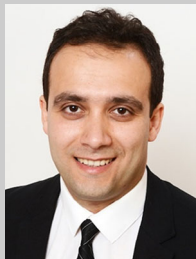
- [5] B. B. Tomazic, Z. Kardiol. **2001**, 90, 68.
- [6] P. Chatterjee, A. Chakraborty, A. K. Mukherjee, *Spectrochim. Acta Part A Mol. Biomol. Spectrosc.* **2018**, 200, 33.
- [7] H. Deng, W. Zheng, J. Jankovic, *Ageing Res. Rev.* **2015**, 22, 20.
- [8] N. Jensen, H. D. Schrøder, E. K. Hejbøl, J. S. Thomsen, A. Brül, F. T. Larsen, M. C. Vinding, D. Orłowski, E.-M. Füchtbauer, J. R. Oliveira, *Am. J. Pathol.* **2018**, 188, 1865.
- [9] Y. Zarb, U. Weber-Stadlbauer, D. Kirschenbaum, D. R. Kindler, J. Richetto, D. Keller, R. Rademakers, D. W. Dickson, A. Pasch, T. Byzova, *Brain* **2019**, 142, 885.
- [10] N. Hishikawa, Y. Hashizume, N. Ujihira, Y. Okada, M. Yoshida, G. Sobue, *Neuropathol. Appl. Neurobiol.* **2003**, 29, 280.
- [11] E. Beniash, J. P. Simmer, H. C. Margolis, *J. Dent. Res.* **2012**, 91, 967.
- [12] S. Elsharkawy, M. Al-Jawad, M. F. Pantano, E. Tejada-Montes, K. Mehta, H. Jamal, S. Agarwal, K. Shuturminska, A. Rice, N. V. Tarakina, *Nat. Commun.* **2018**, 9, 2145.
- [13] O. Gourgas, L. D. Muiznieks, D. G. Bello, A. Nanci, S. Sharpe, M. Cerruti, *Biomacromolecules* **2019**, 20, 2625.
- [14] G. Griffanti, S. N. Nazhat, *Int. Mater. Rev.* **2020**, 65, 502.
- [15] A. L. Boskey, E. Villarreal-Ramirez, *Matrix Biol.* **2016**, 52, 43.
- [16] S. Bertazzo, E. Gentleman, *Eur. Heart J.* **2017**, 38, 1189.
- [17] R. Florencio-Silva, G. R. da S. Sasso, E. Sasso-Cerri, M. J. Simões, P. S. Cerri, *Biomed Res. Int.* **2015**, 2015, 421746.
- [18] T. E. Popowics, J. M. Rensberger, S. W. Herring, *Arch. Oral Biol.* **2004**, 49, 595.
- [19] N. Reznikov, J. A. M. Steele, P. Fratzl, M. M. Stevens, *Nat. Rev. Mater.* **2016**, 1, 1.
- [20] M. Tölle, A. Reshetnik, M. Schuchardt, M. Höhne, M. van der Giet, *Eur. J. Clin. Invest.* **2015**, 45, 976.
- [21] J.-H. Chen, C. A. Simmons, *Circ. Res.* **2011**, 108, 1510.
- [22] W. G. Goodman, G. London, K. Amann, G. A. Block, C. Giachelli, K. A. Hruska, M. Ketteler, A. Levin, Z. Massy, D. A. McCarron, *Am. J. Kidney Dis.* **2004**, 43, 572.
- [23] R. Shroff, D. A. Long, C. Shanahan, *J. Am. Soc. Nephrol.* **2013**, 24, 179.
- [24] M. V. Gomez-Stallons, J. T. Tretter, K. Hassel, O. Gonzalez-Ramos, D. Amofa, N. J. Ollberding, W. Mazur, J. K. Choo, J. M. Smith, D. J. Kereiakes, *Heart* **2019**, 105, 1616.
- [25] C. I. Fisher, J. Chen, W. D. Merryman, *Biomech. Model. Mechanobiol.* **2013**, 12, 5.
- [26] D. C. Sung, C. J. Bowen, K. A. Vaidya, J. Zhou, N. Chapurin, A. Recknagel, B. Zhou, J. Chen, M. Kotlikoff, J. T. Butcher, *Arterioscler., Thromb., Vasc. Biol.* **2016**, 36, 1627.
- [27] J. Chen, J. R. Peacock, J. Branch, W. David Merryman, *J. Biomech. Eng.* **2015**, 137, 020903.
- [28] E. Tsolaki, S. Bertazzo, *Materials (Basel)*. **2019**, 12, 3126.
- [29] R. F. Weska, C. G. Aimoli, G. M. Nogueira, A. A. Leirner, M. J. S. Maizato, O. Z. Higa, B. Polakiewicz, R. N. M. Pitombo, M. M. Beppu, *Artif. Organs* **2010**, 34, 311.
- [30] N. M. Rajamannan, M. Subramaniam, D. Rickard, S. R. Stock, J. Donovan, M. Springett, T. Orszulak, D. A. Fullerton, A. J. Tajik, R. O. Bonow, *Circulation* **2003**, 107, 2181.
- [31] D. Mikroulis, D. Mavrilas, J. Kapalos, P. G. Koutsoukos, C. Lolas, *J. Mater. Sci. Mater. Med.* **2002**, 13, 885.
- [32] C. Delogne, P. V. Lawford, S. M. Habesch, V. A. Carolan, *J. Microsc.* **2007**, 228, 62.
- [33] N. Reznikov, M. Bilton, L. Lari, M. M. Stevens, R. Kröger, *Science (80-)*. **2018**, 360, eaao2189.
- [34] F. Granados-Correa, *Rev. Int.* **2010**, 26, 129.
- [35] E. A. McNally, H. P. Schwarcz, G. A. Botton, A. L. Arsenaault, *PLoS One* **2012**, 7, e29258.
- [36] X. Su, K. Sun, F. Z. Cui, W. J. Landis, *Bone* **2003**, 32, 150.
- [37] M. J. Duer, T. Frišćić, D. Proudfoot, D. G. Reid, M. Schoppet, C. M. Shanahan, J. N. Skepper, E. R. Wise, *Arterioscler., Thromb., Vasc. Biol.* **2008**, 28, 2030.
- [38] W. Karwowski, B. Naumnik, M. Szczepański, M. Myśliwiec, *Med. Sci. Monit. Int. Med. J. Exp. Clin. Res.* **2012**, 18, RA1.
- [39] K. L. Cloyd, I. El-Hamamsy, S. Boonrungsiman, M. Hedegaard, E. Gentleman, P. Sarathchandra, F. Colazzo, M. M. Gentleman, M. H. Yacoub, A. H. Chester, *PLoS One* **2012**, 7, e48154.
- [40] M. Valente, U. Bortolotti, G. Thiene, *Am. J. Pathol.* **1985**, 119, 12.
- [41] Y. Zhao, A. L. Urganus, L. Spevak, S. Shrestha, S. B. Doty, A. L. Boskey, L. M. Pachman, *Calcif. Tissue Int.* **2009**, 85, 267.
- [42] J.-H. Chen, C. Y. Yip, E. D. Sone, C. A. Simmons, *Am. J. Pathol.* **2009**, 174, 1109.
- [43] P. M. Taylor, P. Batten, N. J. Brand, P. S. Thomas, M. H. Yacoub, *Int. J. Biochem. Cell Biol.* **2003**, 35, 113.
- [44] O. Gourgas, J. Marulanda, P. Zhang, M. Murshed, M. Cerruti, *Arterioscler., Thromb., Vasc. Biol.* **2018**, 38, 363.
- [45] S. V. Dorozhkin, *J. Mater. Sci.* **2007**, 42, 1061.
- [46] S. N. Danilchenko, V. N. Kuznetsov, A. S. Stanislavov, A. N. Kalinkevich, V. V. Starikov, R. A. Moskalenko, T. G. Kalinichenko, A. V. Kochenko, J. Lü, J. Shang, *Cryst. Res. Technol.* **2013**, 48, 153.
- [47] M. Pilarczyk, K. Czamara, M. Baranska, J. Natorska, P. Kapusta, A. Undas, A. Kaczor, *J. Raman Spectrosc.* **2013**, 44, 1222.
- [48] J. D. Reid, M. E. Andersen, *Atherosclerosis* **1993**, 101, 213.
- [49] M. C. F. Magalhães, P. Marques, R. N. Correia, *Biomaterialization Asp. Solubility*, John Wiley Sons, Chichester **2006**, p. 71.
- [50] M. Hamad, J.-C. Heughebaert, *J. Cryst. Growth* **1986**, 79, 192.
- [51] A. Y. F. You, M. S. Bergholt, J.-P. St-Pierre, W. Kit-Anan, I. J. Pence, A. H. Chester, M. H. Yacoub, S. Bertazzo, M. M. Stevens, *Sci. Adv.* **2017**, 3, e1701156.
- [52] S. Agarwal, Doctoral Dissertation, Imperial College London **2017**.
- [53] A. Ficaí, E. Andronescu, G. Voicu, S. Pall, *UPB Sci. Bull. Ser. B* **2010**, 72, 47.
- [54] V. Uvarov, I. Popov, N. Shapur, T. Abdin, O. N. Gofrit, D. Pode, M. Duvdevani, *Environ. Geochem. Health* **2011**, 33, 613.
- [55] H. P. Lee, D. Leong, C. T. Heng, *Urol. Res.* **2012**, 40, 197.
- [56] F. Grases, A. Costa-Bauzá, R. M. Prieto, A. Conte, A. Servera, *BMC Urol.* **2013**, 13, 14.
- [57] E. Letavernier, D. Bazin, M. Daudon, *Comptes Rendus Chim.* **2016**, 19, 1456.
- [58] M. D. McKee, A. Nancl, S. R. Khan, *J. Bone Miner. Res.* **1995**, 10, 1913.
- [59] N. Jensen, H. D. Schrøder, E. K. Hejbøl, E.-M. Füchtbauer, J. R. M. de Oliveira, L. Pedersen, *J. Mol. Neurosci.* **2013**, 51, 994.
- [60] F. G. Celzo, C. Venstermans, F. De Belder, J. Van Goethem, L. van den Hauwe, T. van der Zijden, M. Voormolen, T. Menovsky, A. Maas, P. M. Parizel, *Insights Imaging* **2013**, 4, 625.
- [61] K. M. Earle, *J. Neuropathol. Exp. Neurol.* **1965**, 24, 108.
- [62] C. R. Bayliss, N. L. Bishop, R. C. Fowler, *Br. Med. J.* **1985**, 291, 1758.
- [63] B. J. M. Diehl, *Cell Tissue Res.* **1978**, 195, 359.
- [64] T. Kodaka, R. Mori, K. Debari, M. Yamada, *Microscopy* **1994**, 43, 307.
- [65] J. L. Kirschvink, A. Kobayashi-Kirschvink, B. J. Woodford, *Proc. Natl. Acad. Sci.* **1992**, 89, 7683.
- [66] B. A. Maher, I. A. M. Ahmed, V. Karloukovski, D. A. MacLaren, P. G. Foulds, D. Allsop, D. M. A. Mann, R. Torres-Jardón, L. Calderon-Garciduenas, *Proc. Natl. Acad. Sci.* **2016**, 113, 10797.
- [67] C. M. Gohr, M. Fahey, A. K. Rosenthal, *Connect. Tissue Res.* **2007**, 48, 286.
- [68] S. B. L. Low, A. P. Toms, *Eur. J. Radiol. Open* **2019**, 6, 101.

- [69] J. Hamada, W. Ono, K. Tamai, K. Saotome, T. Hoshino, *J. Rheumatol.* **2001**, *28*, 809.
- [70] R. E. Wuthier, L. N. Y. Wu, G. R. Sauer, B. R. Genge, T. Yoshimori, Y. Ishikawa, *Bone Miner.* **1992**, *17*, 290.
- [71] B. D. Boyan-Salyers, J. J. Vogel, L. J. Riggan, F. Summers, R. E. Howell, *Metab. Bone Dis. Relat. Res.* **1978**, *1*, 143.
- [72] D. S. Siegal, J. S. Wu, J. S. Newman, J. L. Del Cura, M. G. Hochman, *Can. Assoc. Radiol. J.* **2009**, *60*, 263.
- [73] W. Y. Chou, C. J. Wang, K. T. Wu, Y. J. Yang, J. Y. Ko, K. K. Siu, *Bone Joint J.* **2017**, *99*, 1643.
- [74] V. Sansone, E. Maiorano, A. Galluzzo, V. Pascale, *Orthop. Res. Rev.* **2018**, *10*, 63.
- [75] M. Naseem, J. Murray, J. F. Hilton, J. Karamchandani, D. Muradali, H. Faragalla, C. Polenz, D. Han, D. C. Bell, C. Brezden-Masley, *BMC Cancer* **2015**, *15*, 1.
- [76] N. Vidavsky, J. A. M. R. Kunitake, L. A. Estroff, *Adv. Healthcare Mater.* **2021**, *10*, 2001271.
- [77] A. Bellahcene, V. Castronovo, *Am. J. Pathol.* **1995**, *146*, 95.
- [78] R. Vanna, C. Morasso, B. Marcinnò, F. Piccotti, E. Torti, D. Altamura, S. Albasini, M. Agozzino, L. Villani, L. Sorrentino, *Cancer Res.* **2020**, *80*, 1762.
- [79] J. A. M. R. Kunitake, S. Choi, K. X. Nguyen, M. M. Lee, F. He, D. Sudilovsky, P. G. Morris, M. S. Jochelson, C. A. Hudis, D. A. Muller, *J. Struct. Biol.* **2018**, *202*, 25.
- [80] A. S. Haka, K. E. Shafer-Peltier, M. Fitzmaurice, J. Crowe, R. R. Dasari, M. S. Feld, *Cancer Res.* **2002**, *62*, 5375.
- [81] L. Wang, G. H. Nancollas, *Chem. Rev.* **2008**, *108*, 4628.
- [82] M. A. Durán-Olivencia, P. Yatsyshin, S. Kalliadasis, J. F. Lutsko, *New J. Phys.* **2018**, *20*, 83019.
- [83] E. Radvar, H. S. Azevedo, *ACS Biomater. Sci. Eng.* **2019**, *5*, 4646.
- [84] M. Murshed, T. Schinke, M. D. McKee, G. Karsenty, *J. Cell Biol.* **2004**, *165*, 625.
- [85] A. Tanimura, D. H. McGregor, H. C. Anderson, *Proc. Soc. Exp. Biol. Med.* **1983**, *172*, 173.
- [86] A. N. Kapustin, J. D. Davies, J. L. Reynolds, R. McNair, G. T. Jones, A. Sidibe, L. J. Schurgers, J. N. Skepper, D. Proudfoot, M. Mayr, *Circ. Res.* **2011**, *109*, e1.
- [87] K. Kohri, S. Nomura, Y. Kitamura, T. Nagata, K. Yoshioka, M. Iguchi, T. Yamate, T. Umekawa, Y. Suzuki, H. Sinohara, *J. Biol. Chem.* **1993**, *268*, 15180.
- [88] X. Lu, B. Gao, T. Yasui, Y. Li, T. Liu, X. Mao, M. Hirose, Y. Wu, D. Yu, Q. Zhu, *Kidney Blood Press. Res.* **2013**, *37*, 15.
- [89] F. Atmani, S. R. Khan, *J. Am. Soc. Nephrol.* **1999**, *10*, S385.
- [90] L. Mo, H.-Y. Huang, X.-H. Zhu, E. Shapiro, D. L. Hasty, X.-R. Wu, *Kidney Int.* **2004**, *66*, 1159.
- [91] B. Yang, X. Lu, Y. Li, Y. Li, D. Yu, W. Zhang, C. Duan, K. Taguchi, T. Yasui, K. Kohri, *Oxid. Med. Cell. Longev.* **2019**, *2019*, 9307256.
- [92] M. Abedin, Y. Tintut, L. L. Demer, *Arterioscler., Thromb., Vasc. Biol.* **2004**, *24*, 1161.
- [93] R. C. Johnson, J. A. Leopold, J. Loscalzo, *Circ. Res.* **2006**, *99*, 1044.
- [94] M. Kagayama, Y. Sasano, I. Mizoguchi, N. Kamo, I. Takahashi, H. Mitani, *J. Periodontal Res.* **1996**, *31*, 229.
- [95] I. Mizoguchi, I. Takahashi, Y. Sasano, M. Kagayama, H. Mitani, *Anat. Embryol. (Berl.)* **1997**, *195*, 127.
- [96] J. L. Reynolds, A. J. Joannides, J. N. Skepper, R. McNair, L. J. Schurgers, D. Proudfoot, W. Jahnhen-Dechent, P. L. Weissberg, C. M. Shanahan, *J. Am. Soc. Nephrol.* **2004**, *15*, 2857.
- [97] J. L. Reynolds, J. N. Skepper, R. McNair, T. Kasama, K. Gupta, P. L. Weissberg, W. Jahnhen-Dechent, C. M. Shanahan, *J. Am. Soc. Nephrol.* **2005**, *16*, 2920.
- [98] J. D. Hutcheson, C. Goettsch, S. Bertazzo, N. Maldonado, J. L. Ruiz, W. Goh, K. Yabusaki, T. Faits, C. Bouten, G. Franck, *Nat. Mater.* **2016**, *15*, 335.
- [99] K. E. Watson, K. Boström, R. Ravindranath, T. Lam, B. Norton, L. L. Demer, *J. Clin. Invest.* **1994**, *93*, 2106.
- [100] Y. Sun, C. H. Byon, K. Yuan, J. Chen, X. Mao, J. M. Heath, A. Javed, K. Zhang, P. G. Anderson, Y. Chen, *Circ. Res.* **2012**, *111*, 543.
- [101] A. Shioi, Y. Nishizawa, S. Jono, H. Koyama, M. Hosoi, H. Morii, *Arterioscler., Thromb., Vasc. Biol.* **1995**, *15*, 2003.
- [102] J. D. Hutcheson, C. Goettsch, T. Pham, M. Iwashita, M. Aikawa, S. A. Singh, E. Aikawa, *J. Extracell. Vesicles* **2014**, *3*, 25129.
- [103] J. D. Hutcheson, J. Chen, M. K. Sewell-Loftin, L. M. Ryzhova, C. I. Fisher, Y. R. Su, W. D. Merryman, *Arterioscler., Thromb., Vasc. Biol.* **2013**, *33*, 114.
- [104] K. Boström, K. E. Watson, S. Horn, C. Wortham, I. M. Herman, L. L. Demer, *J. Clin. Invest.* **1993**, *91*, 1800.
- [105] S. Hirota, M. Imakita, K. Kohri, A. Ito, E. Morii, S. Adachi, H. M. Kim, Y. Kitamura, C. Yutani, S. Nomura, *Am. J. Pathol.* **1993**, *143*, 1003.
- [106] C. M. Shanahan, N. R. Cary, J. C. Metcalfe, P. L. Weissberg, *J. Clin. Invest.* **1994**, *93*, 2393.
- [107] C. R. Dhore, J. P. M. Cleutjens, E. Lutgens, K. B. J. M. Cleutjens, P. P. M. Geusens, P. J. Kitslaar, J. H. M. Tordoir, H. M. H. Spronk, C. Vermeer, M. J. A. P. Daemen, *Arterioscler., Thromb., Vasc. Biol.* **2001**, *21*, 1998.
- [108] P. A. Price, M. R. Urist, Y. Otawara, *Biochem. Biophys. Res. Commun.* **1983**, *117*, 765.
- [109] A. F. Zebboudj, M. Imura, K. Boström, *J. Biol. Chem.* **2002**, *277*, 4388.
- [110] A. F. Zebboudj, V. Shin, K. Boström, *J. Cell. Biochem.* **2003**, *90*, 756.
- [111] S. Mizuiri, Y. Nishizawa, K. Yamashita, K. Ono, T. Naito, C. Tanji, K. Usui, S. Doi, T. Masaki, K. Shigemoto, *Ren. Fail.* **2019**, *41*, 770.
- [112] M. Shen, P. Marie, D. Farge, S. Carpenter, C. de Poelak, M. Hott, L. Chen, B. Martinet, A. Carpentier, *Compt. R. Acad. Sci.* **1997**, *320*, 49.
- [113] D. T. Denhardt, X. Guo, *FASEB J.* **1993**, *7*, 1475.
- [114] C. M. Giachelli, N. Bae, M. Almeida, D. T. Denhardt, C. E. Alpers, S. M. Schwartz, *J. Clin. Invest.* **1993**, *92*, 1686.
- [115] A. Miyachi, J. Alvarez, E. M. Greenfield, A. Teti, M. Grano, S. Colucci, A. Zamboni-Zallone, F. P. Ross, S. L. Teitelbaum, D. Cheresch, *J. Biol. Chem.* **1991**, *266*, 20369.
- [116] Y.-C. Chien, A. Mansouri, W. Jiang, S. R. Khan, J. J. Gray, M. D. McKee, *J. Struct. Biol.* **2018**, *204*, 131.
- [117] C. Cerini, S. Geider, B. Dussol, C. Hennequin, M. Daudon, S. Veessler, S. Nitsche, R. Boistelle, P. Berthézène, P. Dupuy, *Kidney Int.* **1999**, *55*, 1776.
- [118] W. S. Simonet, D. L. Lacey, C. R. Dunstan, M. Kelley, M.-S. Chang, R. Lüthy, H. Q. Nguyen, S. Wooden, L. Bennett, T. Boone, *Cell* **1997**, *89*, 309.
- [119] J. J. Kaden, S. Bickelhaupt, R. Grobholz, K. K. Haase, A. Sarıkoç, M. Brueckmann, S. Lang, I. Zahn, C. Vahl, S. Hagl, *J. Mol. Cell. Cardiol.* **2004**, *36*, 57.
- [120] M. Herrmann, A. Babler, I. Moshkova, F. Gremse, F. Kiessling, U. Kusebauch, V. Nelea, R. Kramann, R. L. Moritz, M. D. McKee, *PLoS One* **2020**, *15*, e0228503.
- [121] D. Stejskal, M. Karpisek, R. Vrtal, V. Student, P. Solichova, R. Fiala, P. Stejskal, *BJU Int.* **2008**, *101*, 1151.
- [122] O. Bilgir, L. Kebapçilar, F. Bilgir, G. Bozkaya, Y. Yildiz, P. Pinar, A. Tastan, *Intern. Med.* **2010**, *49*, 1281.
- [123] W. C. O'neill, K. A. Lomashvili, H. H. Malluche, M.-C. Faugere, B. L. Riser, *Kidney Int.* **2011**, *79*, 512.
- [124] V. P. Persy, M. D. McKee, *Kidney Int.* **2011**, *79*, 490.
- [125] M. S. Tung, B. Tomazic, W. E. Brown, *Arch. Oral Biol.* **1992**, *37*, 585.

- [126] A. C. S. Tan, M. Pilgrim, S. Fearn, S. Bertazzo, E. Tsolaki, A. P. Morrell, M. Li, J. Messinger, R. Dolz-Marco, J. Lei, *Invest. Ophthalmol. Vis. Sci.* **2018**, *59*, 2433.
- [127] J. Kawaguchi, I. Kii, Y. Sugiyama, S. Takeshita, A. Kudo, *J. Bone Miner. Res.* **2001**, *16*, 260.
- [128] J. Tsunozumi, H. Sugiura, L. Oinam, A. Ali, B. Q. Thang, A. Sada, Y. Yamashiro, M. Kuro-O, H. Yanagisawa, *Matrix Biol.* **2018**, *74*, 5.
- [129] J. Moradian-Oldak, *Front. Biosci. J. Virtual Libr.* **2012**, *17*, 1996.
- [130] M. R. H. Krebs, E. H. C. Bromley, S. S. Rogers, A. M. Donald, *Biophys. J.* **2005**, *88*, 2013.
- [131] C. Exley, E. House, J. F. Collingwood, M. R. Davidson, D. Cannon, A. M. Donald, *J. Alzheimer's Dis.* **2010**, *20*, 1159.
- [132] F. Chiti, C. M. Dobson, *Annu. Rev. Biochem.* **2006**, *75*, 333.
- [133] K. M. M. Carneiro, H. Zhai, L. Zhu, J. A. Horst, M. Sitlin, M. Nguyen, M. Wagner, C. Simpliciano, M. Milder, C.-L. Chen, *Sci. Rep.* **2016**, *6*, 1.
- [134] L.-W. Jin, K. A. Claborn, M. Kurimoto, M. A. Geday, I. Maezawa, F. Sohrawy, M. Estrada, W. Kaminsky, B. Kahr, *Proc. Natl. Acad. Sci.* **2003**, *100*, 15294LP.
- [135] J. D. Hartgerink, E. Beniash, S. I. Stupp, *Science (80-)*. **2001**, *294*, 1684.
- [136] E. Radvar, H. S. Azevedo, *Macromol. Biosci.* **2018**, *19*, 1800221.
- [137] C. Wang, K. Jiao, J. Yan, M. Wan, Q. Wan, L. Breschi, J. Chen, F. R. Tay, L. Niu, *Prog. Mater. Sci.* **2020**, *5*, 100712.
- [138] N. Nassif, N. Gehrke, N. Pinna, N. Shirshova, K. Tauer, M. Antonietti, H. Cölfen, *Angew. Chem., Int. Ed.* **2005**, *44*, 6004.
- [139] K. Imachi, T. Chinzei, Y. Abe, K. Mabuchi, H. Matsuura, T. Karita, K. Iwasaki, S. Mochizuki, Y. Son, I. Saito, *J. Artif. Organs* **2001**, *4*, 74.
- [140] G. M. Bernacca, T. G. Mackay, R. Wilkinson, D. J. Wheatley, *Biomaterials* **1995**, *16*, 279.
- [141] A. G. Kidane, G. Burriesci, M. Edirisinghe, H. Ghanbari, P. Bonhoeffer, A. M. Seifalian, *Acta Biomater.* **2009**, *5*, 2409.
- [142] G. Thirivikraman, S. L. Johnson, Z. H. Syedain, H. S. Lee, R. T. Tranquillo, *Acta Biomater.* **2020**, *110*, 164.
- [143] E. J. Farrar, V. Pramili, J. M. Richards, C. Z. Mosher, J. T. Butcher, *Biomaterials* **2016**, *105*, 25.
- [144] Y. Wang, T. Azaïs, M. Robin, A. Vallée, C. Catania, P. Legriel, G. Pehau-Arnaudet, F. Babonneau, M.-M. Giraud-Guille, N. Nassif, *Nat. Mater.* **2012**, *11*, 724.
- [145] G. Griffanti, E. Rezabeigi, J. Li, M. Murshed, S. N. Nazhat, *Adv. Funct. Mater.* **2020**, *30*, 1903874.
- [146] J. M. Richards, J. A. M. R. Kunitake, H. B. Hunt, A. N. Wnorowski, D. W. Lin, A. L. Boskey, E. Donnelly, L. A. Estroff, J. T. Butcher, *Acta Biomater.* **2018**, *71*, 24.
- [147] B. C. Starcher, D. W. Urry, *Biochem. Biophys. Res. Commun.* **1973**, *53*, 210.
- [148] S. Roberts, M. Dzuricky, A. Chilkoti, *FEBS Lett.* **2015**, *589*, 2477.
- [149] A. L. Boskey, B. D. Boyan, Z. Schwartz, *Calcif. Tissue Int.* **1997**, *60*, 309.
- [150] S. Ahmed, M. M. Hasan, Z. A. Mahmood, *J. Pharmacogn. Phytochem.* **2016**, *5*, 28.
- [151] D. S. Frank, A. H. Aldoukhi, W. W. Roberts, K. R. Ghani, A. J. Matzger, *ACS Biomater. Sci. Eng.* **2019**, *5*, 4970.
- [152] S. P. Pathi, D. D. W. Lin, J. R. Dorvee, L. A. Estroff, C. Fischbach, *Biomaterials* **2011**, *32*, 5112.
- [153] S. Choi, S. Coonrod, L. Estroff, C. Fischbach, *Acta Biomater.* **2015**, *24*, 333.
- [154] S. O'Grady, M. P. Morgan, *Sci. Rep.* **2019**, *9*, 1.
- [155] S. Bersini, J. S. Jeon, G. Dubini, C. Arrigoni, S. Chung, J. L. Charest, M. Moretti, R. D. Kamm, *Biomaterials* **2014**, *35*, 2454.
- [156] M. Cavo, M. Fato, L. Peñuela, F. Beltrame, R. Raiteri, S. Scaglione, *Sci. Rep.* **2016**, *6*, 1.
- [157] J. Salgado, O. P. Coutinho, R. L. Reis, *Macromol. Biosci.* **2004**, *4*, 743.
- [158] E. Asenath-Smith, H. Li, E. C. Keene, Z. W. Seh, L. A. Estroff, *Adv. Funct. Mater.* **2012**, *22*, 2891.
- [159] T. D. Sargeant, C. Aparicio, J. E. Goldberger, H. Cui, S. I. Stupp, *Acta Biomater.* **2012**, *8*, 2456.
- [160] D. Bazin, C. Jouanneau, S. Bertazzo, C. Sandt, A. Dessombz, M. Réfrégiers, P. Dumas, J. Frederick, J.-P. Haymann, E. Letavernier, *Compt. R. Chim.* **2016**, *19*, 1439.
- [161] Y. Li, T. T. Thula, S. Jee, S. L. Perkins, C. Aparicio, E. P. Douglas, L. B. Gower, *Biomacromolecules* **2012**, *13*, 49.
- [162] N. Reznikov, R. Shahar, S. Weiner, *Acta Biomater.* **2014**, *10*, 3815.
- [163] E. House, K. Jones, C. Exley, *J. Alzheimer's Dis.* **2011**, *25*, 43.



Elham Radvar received her B.Sc. degree in Chemical Engineering from Urmia University of Technology, Iran in 2012. In 2019, she completed her Ph.D. in Biomedical Engineering under the supervision of Dr. Helena Azevedo at Queen Mary University of London. Elham is currently working in a postdoctoral role at the Centre for Oral, Clinical and Translational Sciences, Faculty of Dentistry at King's College London (KCL). Her research focuses on developing dental biomaterials based on recombinant proteins to create hierarchical structures.



Sherif Elsharkawy holds a Bachelor of Dental Surgery (BDS) from the Faculty of Dentistry with honors at Alexandria University, Egypt. He completed his M.S. at Barts and The London School of Medicine and Dentistry followed by a Ph.D. and postdoctoral fellowship with Prof. Alvaro Mata in the Institute of Bioengineering at Queen Mary University of London. He is currently a Clinical Lecturer in Prosthodontics at the Centre for Oral, Clinical and Translational Sciences, Faculty of Dentistry, Oral & Craniofacial Sciences at King's College London (KCL). His research lab is highly interdisciplinary and collaborative, focusing on understanding biomineralization processes and developing bio-inspired hierarchical materials for various biomedical and dental applications.